

**SEQUENCE STRATIGRAPHY, STRUCTURE AND TECTONIC SETTING
OF AN INTRA-ARC STRIKE-SLIP BASIN
(BISBEE BASIN, SOUTHERN ARIZONA)**

Bassett, Kari N., Dept. of Geological Sciences, Univ. of Canterbury, Prvt. Bag 4800,
Christchurch, NZ, k.bassett@geol.canterbury.ac.nz (corresponding author)

Busby, Cathy J., Dept. of Geological Sciences, University of California, Santa Barbara,
CA, USA, 93106, cathy@geol.ucsb.edu

ABSTRACT

Sequence stratigraphic models are difficult to apply in strike slip basins, which may “porpoise” along releasing and restraining bends, particularly in nonmarine depositional basins beyond the direct control of accommodation space created by eustasy. Despite this, sequence stratigraphic models have been applied to nonmarine strike slip basins along conservative plate boundaries where the basin fill is siliciclastic. Strike slip basins are also common at convergent plate margins, however, where oblique subduction produces strike slip faults in the thermally-weakened arc. We present here the first sequence stratigraphic analysis of a nonmarine, volcanically-dominated strike slip basin.

The basal deposits of the Bisbee basin in southern Arizona consist of the Late Jurassic (to Early Cretaceous?) Glance Conglomerate and interstratified volcanic rocks, which we interpret to record strain partitioning into a western (outboard) belt of intra-arc strike slip basins and an eastern (inboard) belt of backarc extensional basins. Sequence stratigraphic analysis in the present-day Santa Rita Mountains of the western belt permits

reconstruction of the intra-arc basin in a series of time slices that show the relationship of eight unconformity-bounded sequences to high-angle intrabasinal faults, which alternated between normal-slip separation and reverse-slip separation. Five of the eight unconformities show extreme vertical relief (900 – 1800 m) and very high paleo-slope gradients (20° - 71°), with pronounced asymmetry facing away from the master fault toward the basin; these unconformities are interpreted to represent paleo-slide scars produced during basin inversion events. The other three unconformities are more symmetrical, with vertical relief of 300 – 400 m and paleo-slope gradients of 20° to 40° . These probably represent paleocanyons cut during basin inversion events. The scale of these unconformities is enormous compared to published examples from other basin types; similarly, the maximum thicknesses of the unconformity-bounded depositional sequences are unusually great, due to very high rates of subsidence on both intrabasinal and basin-bounding faults. The strike slip basin fill is dominated by small polygenetic, multivent volcanic complexes that we consider to be typical of basins sited on a major fault zone, where strands of the fault frequently plumb small batches of magma to the surface. Because of this, individual volcanic constructs do not grow large enough to provide significant accommodation in volcano-bounded basins.

INTRODUCTION

Application of sequence stratigraphy to tectonically active basins is difficult and models tend to depart from those developed for passive-margin settings (Vail et al., 1977; Jervey, 1988; Van Wagoner et al., 1988). This is particularly true for strike-slip basins, which commonly show subsidence rates of greater than 1 km/Ma (Johnson et al., 1983;

Christie-Blick and Biddle, 1995; Dorsey and Umhoefer, 2000). For example, where accommodation space is dominantly controlled by tectonic subsidence, relative sea level may rise continuously; then, sequence boundaries must be defined by marine flooding surfaces and downlap zones, rather than by unconformities (Dart et al., 1994; Gawthorpe et al., 1994; Burns et al., 1997; Dorsey and Umhoefer, 2000). A further complexity in strike-slip settings is that basins may “porpoise” (Crowell, 1974) due to rapidly alternating structural inversions along releasing and restraining bends; also, extension and shortening may occur simultaneously in different parts of the same basin (Crowell, 1974; Wood et al., 1994; Barnes et al., 2001).

Traditional sequence stratigraphic models are also difficult to apply to depositional systems distal from shorelines and therefore out of the direct control of accommodation space created by eustacy (Posamentier and Vail, 1988). An aggradational/degradational systems tract nomenclature has been developed in response (Currie, 1997). All previous sequence stratigraphic models assume that unconformities are cut by fluvial or shallow marine processes, but in this paper, we describe unconformities that were cut at least in part by landsliding.

Finally, traditional systems tract nomenclature is difficult to apply to volcanic and volcanoclastic deposits due to rapid lateral lithofacies changes, the episodicity of sediment supply (controlled by eruptive style and recurrence rate), and the varying erodability of volcanic products (controlled by eruptive style and composition) (G. Smith, 1991; R. Smith, 1991). Volcanic constructs also modify topography within the basin independent of changes in accommodation space, affecting sequence stratigraphic architecture.

In this paper we develop a sequence stratigraphic model for an intra-arc strike-slip basin in the western part of the Bisbee basin of southern Arizona, in the present-day Santa Rita Mountains (Fig. 1). This is a nonmarine basin that was tectonically very active and dominated by volcanism. Elsewhere, we make process volcanological and sedimentological interpretations of the basin fill, we group cogenetic volcanic and sedimentary lithofacies associations into systems tracts, and we develop a facies model for intra-arc strike slip basins (Busby and Bassett, in review). In this paper, we place volcanic and sedimentary systems tracts into a sequence stratigraphic framework by mapping unconformity-bounded depositional sequences, and by examining the relationships of the unconformities and depositional sequences to intrabasinal and extrabasinal faulting and volcanism. This permits reconstruction of the structural and paleo-geomorphic evolution of the strike slip basin. We then present a model for the Late Jurassic origin of the Bisbee basin, involving strain partitioning into a western (outboard) belt of intra-arc strike slip sub-basins and an eastern (inboard) belt of backarc extensional sub-basins.

This paper represents a first attempt at applying sequence stratigraphic principles to a volcanically-dominated basin.

THE BISBEE BASIN AND THE GLANCE CONGLOMERATE

Regional Tectonic Setting

Throughout much of southern Arizona, Late Jurassic to Early Cretaceous(?) conglomerates and interstratified volcanic rocks occur upsection from more dominantly volcanic sections that are well dated as Early to Middle Jurassic in age (Fig. 1; Saleeby

and Busby-Spera, 1992). These conglomerates are widely referred to as the Glance Conglomerate, and in many places lie at the base of Cretaceous nonmarine to marine sections referred to as the Bisbee Group (Fig. 1; Bilodeau, 1979; Jacques-Ayala, 1995; Lawton and Olmstead, 1995). The Glance Conglomerate is the basal unit in the Bisbee basin and thus records the tectonic setting during the basin's initial opening. It occurs as piedmont fan and canyon fill deposits with locally interbedded lava flows and ignimbrites in grabens, half-grabens, and calderas (Bilodeau, 1979; Dickinson et al., 1987; Busby and Kokelaar, 1992; Lipman and Hagstrum, 1992; Bassett and Busby, 1996a, 1996b, 1997; Lawton and McMillan, 1999).

Some workers have inferred that the Glance Conglomerate forms part of the Jurassic arc sequence, particularly in areas where it has abundant interstratified volcanic rocks (Tosdal et al., 1989; Nourse, 1995), whereas other workers have suggested it records backarc extension (Bilodeau, 1979). Still others have inferred that the Glance Conglomerate records continental rifting associated with the opening of the Gulf of Mexico (Dickinson et al., 1986, 1987; Lawton and McMillan, 1999). A kind of "fence-sitting" model was proposed in which the Gulf of Mexico-related rifts progressively exploited the thermally weakened, structurally attenuated crust of the Jurassic arc (Busby-Spera et al., 1989; Saleeby and Busby-Spera, 1992; Lawton and McMillan, 1999). Strike-slip tectonics related to the Mojave-Sonora megashear of Silver and Anderson (1983) probably influenced this rifting (Bassett and Busby, 1997; Lawton et al., 1997). We propose a different "fence-sitting" model wherein the Glance Conglomerate records oblique convergence partitioned between intra-arc strike slip and back-arc extension.

The eastern part of the Glance Conglomerate outcrop belt, which is "inboard" relative to the paleoPacific subduction margin, contains few interstratified volcanic rocks, and these are basaltic in composition (Lawton and Olmstead, 1995; Lawton and McMillan, 1999). Geochemical data on the basalts from the eastern Bisbee basin indicate eruption in a rift, rather than arc, environment (Lawton and McMillan, 1999).

The Glance Conglomerate on the western, outboard edge of the Bisbee basin contains abundant rhyolitic, dacitic and andesitic volcanic and volcanoclastic deposits interstratified with boulder breccia-conglomerates (Fig. 1). The compositions have been determined almost entirely by phenocryst mineralogy (Hayes and Raup, 1968; Hayes, 1970a; Drewes, 1971c; Kluth, 1982; Lipman and Hagstrum, 1992); however, geochemical analysis was done on volcanic rock samples from the Canelo Hills region (Fig. 1). These show LREE enrichment, Th enrichment and a strong negative Eu anomaly interpreted to record a variation on continental rift volcanism (Krebs and Ruiz, 1987); however, we believe the compositions indicate a volcanic arc setting (using criteria of Saunders and Tarney, 1984; Woodhead et al., 1993).

We have focused our studies in basins along the Sawmill Canyon fault zone in the western Bisbee basin because it is the widest and longest fault zone in the basin (Fig. 1) and it formed an important conduit for andesitic to rhyolitic magmas throughout the Jurassic (Riggs and Busby-Spera, 1990; Busby-Spera and Kokelaar, 1991; Bassett and Busby, 1996b). The Sawmill Canyon fault zone and related NW-trending, steeply-dipping faults form a regional lineament inherited from Precambrian basement, and reactivated in Mesozoic and Cenozoic times (Fig. 1; Titley, 1976; Drewes, 1981). The Jurassic movement history of the Sawmill Canyon fault zone has been variably

interpreted as normal, dextral or sinistral (Drewes, 1972; Titley, 1976; Bilodeau, 1979; Drewes, 1981; Busby-Spera and Kokelaar, 1991; Hagstrum and Lipman, 1991; Lipman and Hagstrum, 1992). This fault marks the northeast structural boundary of thick Early to Middle Jurassic arc volcanic successions, interpreted to form the fill of a 1,000 km long extensional arc graben-depression that extended semicontinuously from Sonora, Mexico, to northern California and Nevada (Busby-Spera, 1988). Evidence for movement on the Sawmill Canyon fault zone in Late Jurassic time includes large slide masses interbedded with the Glance Conglomerate in the Mustang Mountains, the Huachuca Mountains, and the Canelo Hills (Fig. 1; Hayes and Raup, 1968; Davis et al., 1979) as well as along the southern extension of the Sawmill Canyon fault zone into Mexico (McKee and Anderson, 1998). In this paper we present evidence the Sawmill Canyon fault zone was active as a strike slip fault during deposition of the Glance conglomerate and interstratified volcanic rocks in the present-day Santa Rita Mountains (Fig.1).

Glance Conglomerate and Volcanics in the Santa Rita Mountains

Late Jurassic strata of the Santa Rita Mountains were previously mapped as the Temporal, Bathub and Glance Formations, and subdivided into members (Drewes, 1971a). Bilodeau (1979), however, considered these strata to be part of the basal conglomerates of the Bisbee basin (i.e. Glance Conglomerate), and we agree. Our mapping (Fig. 2) shows there is no basis for the distinction of the three formations proposed by Drewes (1971a), let alone individual members. Lithofacies of the three "formations" repeat and interfinger with each other (Fig. 2); furthermore, we map major unconformities that cross-cut Drewes' (1971a) formational and member boundaries (Fig.

2). For these reasons, we informally refer to the Temporal, Bathtub, and Glance Formations in the Santa Rita Mountains as Glance conglomerate and volcanics, while emphasizing that it is more volcanic than sedimentary here. Similarly, the term “Glance tuffs” has been informally used for ignimbrites interstratified with Glance conglomerate elsewhere (Vedder, 1984). Other revisions of previously-published formational boundaries in the Santa Rita Mountains are presented as a geologic map in the data repository (item 1).

The Glance conglomerate and volcanics in the Santa Rita Mountains crop out in a 12.5 x 4 mile elongate belt extending southward from the Sawmill Canyon fault zone (Fig. 2). Beds strike roughly north and dip $\sim 30^\circ$ E toward the NW-SE striking Sawmill Canyon fault zone, producing an oblique cross-section in map view that lies at $\sim 55^\circ$ angle to the regional trend of the fault zone. The top of the Glance conglomerate and volcanics is cut by splays of the Sawmill Canyon fault zone to the northeast, and it is buried by Quaternary gravels to the southeast (Fig. 2).

The Glance conglomerate and volcanics lie unconformably on the Middle Jurassic Mt. Wrightson Formation, the Middle Jurassic Piper Gulch monzonite and the Middle Jurassic Squaw Gulch granite (Fig. 2), all of which were eroded from the substrate (along the basal unconformity) or shed from the Sawmill Canyon fault zone to supply most of the clasts to the breccia-conglomerate beds (Busby and Bassett, in review). Intraformational clasts are also common in the breccia-conglomerates (Busby and Bassett, in review), as expected, given the number and scale of intraformational unconformities (Fig. 2, Table 2).

Age and Possible Regional Correlations

We assign a preferred age of Late Jurassic (and/or latest Middle Jurassic) to the Glance conglomerate and volcanics based on cross-cutting relationships and clast compositions. The underlying Mt. Wrightson Formation dips an average of about 20 degrees more steeply than the Glance conglomerate and volcanics, and it is cut by a deep unconformity that shows more than 1.7 km of vertical relief across the field area (Fig. 2). The uplift that created this unconformity also exposed Jurassic plutonic rocks at the surface before deposition of the Glance conglomerate and volcanics began (unconformity 1, Table 1). Seven out of eight unconformity-bounded depositional sequences of the Glance conglomerate and volcanics have abundant distinctive clasts of Mt. Wrightson red ultrawelded ignimbrite in its breccia-conglomerates. U/Pb zircon dates on abraded and acid-washed zircons, from several samples throughout the Mount Wrightson Formation, indicate that it accumulated from 190 Ma to 170 Ma (Riggs et al., 1993), making the Glance conglomerate and volcanics younger than that. Other distinctive clasts derived from the Mount Wrightson Formation are the clasts of eolian quartz arenite; these clasts are restricted to the northernmost part of the Glance conglomerate and volcanics (Fig. 2) where it onlaps the upper member of the Mount Wrightson Formation, which has by far the highest proportion of interbedded eolian quartz arenite (Riggs and Busby-Spera, 1990).

The Glance conglomerate and volcanics also rests unconformably on the Squaw Gulch granite and the Piper Gulch monzonite (Fig. 2), and it contains abundant clasts of both in seven out of eight depositional sequences. The Piper Gulch monzonite intrudes the lower

member of the Mount Wrightson Formation and is approximately coeval with it (Riggs et al, 1993), with an age of 184 +/- 2 Ma (Asmerom et al., 1990). Intrusive relationships suggest it predates the Squaw Gulch granite (Drewes, 1976), which may thus be Middle Jurassic, although it has not been directly dated.

There are no direct constraints on the upper age limit of the Glance conglomerate and volcanics, but it is inferred to be pre-Cretaceous, because there are no dated Early Cretaceous (pre-Laramide) volcanic (or granitic) rocks in southern Arizona.

To summarize, the Glance conglomerate and volcanics must be younger than the 170 Ma Mt. Wrightson Formation, so its base may be late Middle Jurassic, but if the depth of the basal unconformity (which exposes Jurassic granite) records several million years of erosion, the formation may be entirely Late Jurassic in age. If it is Late Jurassic, it would be fully correlative with the Glance Conglomerate and interbedded basaltic volcanics in the eastern Bisbee basin, which have yielded Late Jurassic, Oxfordian ammonites (Lawton and Olmstead, 1995). If the Glance conglomerate and volcanics is entirely Late Jurassic in age, it would be correlative with a distal (backarc) tuff of the Tidewell Member of the Morrison Formation, dated at 154.8 +/- 0.6 Ma (Bart Kowallis, pers. comm.). If the Glance conglomerate and volcanics is late Middle Jurassic in age, it would make a reasonable source for distal (backarc) tuffs in the upper part of the Carmel Formation, with ages of 166.2 +/- 1.2 and 168.2 +/- 0.5 Ma (Kowallis et al., 2001).

SEQUENCE STRATIGRAPHY AND SYNDEPOSITIONAL FAULTING

We present the sequence stratigraphy of the Glance conglomerate and volcanics by identifying sequence-bounding unconformities, and tracing them into correlative

conformities using detailed lithofacies mapping (Figs. 2). Lithologic descriptions and facies interpretations are presented in Busby and Bassett (in review) and summarized in data repository item 2.

Unconformities within the Glance conglomerate and volcanics are recognized where a distinctive lithologic unit is cut by an erosional surface overlain by an unrelated lithologic unit. This requires detailed volcanic facies analyses, because of very rapid lateral facies changes typical of volcanic systems. Specifically, one must have a good understanding of process volcanology (as well as volcanoclastic and siliciclastic sedimentology), in order to recognize cogenetic tracts of facies, referred to here as “lithofacies associations” or “volcanic systems tracts”. These are analogous to the “systems tracts” of siliclastic systems, defined as “linkage of coeval depositional systems on a given depositional surface” (Brown and Fisher, 1977) or “genetically associated deposits” (Posamentier et al, 1988) or “genetic stratigraphic sequences” (Galloway, 1989). Volcanoclastic facies analysis is a much younger and less widely-applied field of research than siliciclastic facies analysis, so far fewer models exist in the literature. For all of these reasons, our “volcanic systems tracts” are more complex than those used in traditional siliciclastic sequence analysis. They are described and interpreted in Busby and Bassett (in review), and briefly summarized here before we show how they are used to map unconformities and correlative conformities.

Systems Tracts of the Glance Conglomerate and Volcanics

The Glance conglomerate and volcanics in the Santa Rita Mountains was deposited in two sub-basins separated by a structural arch or paleohigh (Fig. 2). It is composed of

volcanic and volcanoclastic rocks interstratified with boulder to cobble breccia-conglomerates grouped into cogenetic lithofacies associations or “volcanic systems tracts” by composition (rhyolitic vs. dacitic vs. andesitic), and by inferred source areas (intrabasinal vs. proximal extrabasinally sourced vs. distal extrabasinally sourced) (data repository item 2; Busby and Bassett, in review).

The two proximal extrabasinally sourced systems tracts were both shed from the Sawmill Canyon fault zone. The first is the boulder breccia-conglomerate lithofacies, and the second is the dacitic block-and-ash-flow tuff lithofacies (data repository item 2; Busby and Bassett, in review). The presence of boulder breccia-conglomerates indicates substantial relief at the time of deposition. The interstratified dacitic block-and-ash-flow tuffs are interpreted to be the products of lava dome collapses, from magmas plumbed up the Sawmill Canyon fault zone.

The intrabasinally-sourced andesitic systems tract consists of intrusions, vulcanian breccias, lava flows, ignimbrites, and reworked vitric tuffs (Fig. 2, data repository item 2). The association of andesitic intrusions with thick successions of andesitic lava flows and vulcanian breccias indicates intrabasinal venting.

The intrabasinally-sourced rhyolitic systems tract includes effusive and explosive subassociations (data repository item 2; Busby and Bassett, in review). For the effusive subassociation, rhyolitic intrusions are mapped directly into the rhyolitic dome and dome breccia lithofacies, and the rhyolitic domes are sited on syn-depositional faults (Fig. 2). The rhyolitic dome-dome breccia lithofacies is fringed by the rhyolitic block-and-ash-flow tuff lithofacies, interpreted to represent pyroclastic flows generated by lava dome collapse. This assemblage is interstratified with the explosive subassociation consisting

of the rhyolitic ignimbrite lithofacies and the rhyolitic plinian-phreatoplinian lithofacies (Fig. 2; Busby and Bassett, in review). Together, these two assemblages record alternating effusive and explosive silicic volcanism within the basin, through vents controlled by syndepositional faulting.

Four types of rhyolitic ignimbrite have been identified as extrabasinally sourced because they differ from the intrabasinal ignimbrites in phenocryst and lithic compositions, and because there are no identified vents, intrusions or other proximal deposits with similar mineralogy within the basin (Busby and Bassett, in review). There are two distinctive quartz-crystal rich ignimbrites, two lithic-rich ignimbrites (one with distinctive limestone lithics) and two red, high-grade ignimbrites (Fig 2; Busby and Bassett, in review). The extrabasinally-sourced rhyolitic ignimbrites occur largely in the southern sub-basin but some spill over the paleohigh for a short distance into the northern sub-basin. Each of these ignimbrites is restricted to one or two stratigraphic levels; this fact, and their distinctive textures and compositions, make them useful marker horizons that help to tie together the sequences of the northern and southern sub-basins. These were most likely outflow ignimbrites erupted from calderas elsewhere in the Bisbee basin (Busby and Kokelaar, 1992; Bassett and Busby, in review).

Use of “Volcanic Systems Tracts” to Identify Unconformities and Correlative Conformities

Unconformities are most easily identified where they cut distinctive, widespread lithofacies; similarly, their continuation into correlative conformities is easiest where distinctive, widespread lithofacies are involved. Intrabasinally-sourced units that are

widespread include the rhyolitic plinian-phreatoplinian lithofacies; the andesitic ignimbrites; and the rhyolitic white high-grade ignimbrite (Fig. 2, data repository item 2). Extrabasinally-sourced volcanic lithofacies that are widespread include the rhyolitic crystal-rich ignimbrites; the rhyolitic lithic-rich ignimbrite; and the upper rhyolitic red high-grade ignimbrite (Fig. 2, data repository item 2). Lithofacies associations (“volcanic systems tracts”) described above are also useful for mapping unconformities and their correlative conformities.

Another type of “systems tract” available to volcanic stratigraphers is the use of compositional packages. The intrabasinal volcanic units of the Glance conglomerate and volcanics alternate between silicic and intermediate, and the only silicic units interstratified with the andesites are the extrabasinally-sourced ignimbrites and the plinian-phreatoplinian tuffs, which are by nature both widespread. Andesites are by nature far less extensive than explosive silicic volcanic rocks, and we can map all of our andesite units save one (the vulcanian breccia) directly into an intrusive equivalent (Fig. 2); that is, they are all intrabasinal. Each andesite lithofacies association therefore forms a “genetic stratigraphic sequence”, consisting of a core area of andesitic lava flows, flow breccias and intrusions, surrounded by any or all of the other three andesitic lithofacies (vulcanian breccias, ignimbrites, and vitric tuffs and tuffaceous sandstones; (Fig. 2, data repository item 2; Busby and Bassett, in review).

There are two types of lithofacies that pose serious difficulties when we project unconformities through correlative conformable sections. Unconformities and depositional sequences cannot be mapped continuously through the intrusive lithofacies (Fig. 2). This is more of a problem in areas of lower accommodation, where depositional

sequences are “condensed” and therefore harder to recognize, than it is in areas of higher accommodation, where depositional sequences are “expanded”. For example, the andesite laccolithic intrusions in the paleohigh (structural arch) between the northern and southern sub-basins obscure a greater number of depositional sequences than the rhyolite intrusion at the base of the northern sub-basin (Fig. 2). Although the intrusions can be a nuisance for this reason, they are very useful for recognition of fault-controlled, intrabasinal volcanism. The second major type of lithofacies that can pose difficulties in projection of unconformities through correlative conformable sections is the boulder breccia-conglomerate lithofacies, which forms amalgamated monolithologic sections up to 1.1 km thick (close to the Sawmill Canyon fault zone, Fig. 2, data repository item 2). Fortunately, there are enough intervening mappable units to divide the remaining 2 km of that boulder breccia-conglomerate section into four parts (Fig. 2). The boulder breccia-conglomerate lithofacies is useful for correlation only where relatively thin horizons (interstratified with other lithofacies types) extend further into the basin.

To summarize, this is the first attempt we are aware of to apply sequence analysis to a volcanically-dominated basin. It would be impossible to subdivide the Glance conglomerate and volcanics into cogenetic sequences (“systems tracts”) without mapping and correlating unconformities and correlative conformities, but it would also be impossible to map and correlate unconformities without understanding the systems tracts. We hope that the methods used here, and in Busby and Bassett (in review), will be applied to the interpretation of other volcanically dominated basins in the geologic record, but we warn the reader that this study would have been impossible without excellent exposure.

Time Slices Defined by Unconformity-Bound Sequences

We present cross-sectional views of the basin, divided into eight time slices defined by unconformity-bound depositional sequences (Fig. 3). The Gringo Gulch fault zone appears on all of the time slices except the first; the trend of this E-W, subvertical fault is approximately perpendicular to the N-S strike of the Glance conglomerate and volcanics basin fill and is an echelon to the Sawmill Canyon fault zone. Because the Sawmill Canyon fault zone trends at a 55 degree angle to the strike of the basin fill, it does not coincide with the boundary to the northern basin margin in the cross sectional view afforded by present-day exposures, but instead lies about a kilometer to the north on the map view (Fig. 2). In the third dimension, however, (projecting eastward) it must have approached the north end of the preserved basin fill within a few hundred meters. The Sawmill Canyon fault zone is inferred to be the dominant basin-bounding fault, because total subsidence increases toward it, and intrabasinal, syndepositional faults show the greatest displacement near it (Fig. 3). The Sawmill Canyon fault zone was clearly reactivated during the Late Cretaceous to Early Tertiary Laramide Orogeny, because it cuts the top of the Glance conglomerate and volcanics and juxtaposes fault slivers of Late Cretaceous (and older) strata against it (Fig. 2).

Our sequence stratigraphic “time slice” approach allows us to identify syndepositional high-angle faults, and show that some of these alternated between dip-slip and reverse-slip offset, and that at times, reverse faults were active synchronously with normal faults elsewhere in the basin.

Unconformity 1 and Sequence 1

Unconformity 1 is one of the three deepest unconformities (Table 1, Fig. 2), with vertical relief of 1.7 km, lateral extent of at least 6 km, and slope gradients of up to 71 degrees. The scale of the erosion indicates that it was controlled by tectonic uplift. This uplift must have been greatest in the south, progressively decreasing toward the north, because Middle Jurassic plutons and the Lower Jurassic lower member of the Mount Wrightson Formation were brought to the surface in the south, whereas the Middle Jurassic middle member of the Mount Wrightson Formation forms the basin floor in the north (compare our Fig. 2 with Fig. 2 of Riggs and Busby-Spera, 1990).

Sequence 1 records the creation of accommodation in the north half of the field area (Figs. 2, 3). This was probably accomplished by subsidence of two fault-bounded troughs, each about 1.5 km deep. The faults bounding these two troughs are not exposed, because this part of the range has the only forest cover on the Glance conglomerate and volcanics, but the units comprising the fill of the two troughs (described here) are resistant to erosion, and are well exposed. We infer that they represent fault-bounded troughs because of their extremely narrow and deep geometry, and by analogy with fault-bounded troughs in the rest of the Glance conglomerate and volcanics, which is very well exposed. The map of the underlying Mount Wrightson Formation (Riggs and Busby-Spera, 1990) permits this interpretation.

Depositional sequence 1 begins with a widespread rhyolitic plinian-phreatoplinian tuff, which allows us to correlate the basal strata between the two fault-bounded troughs. Then a rhyolite lava dome grew in the southern fault-bounded trough while 0.7 km thick, boulder breccia-conglomerates began to fill the northern fault-bounded trough. This was

followed by a second rhyolitic plinian-phreatoplinian eruption, with a more marked phreatoplinian signature than the first (dominantly plinian) tuff, providing another timeline between the northern and southern fault-bounded troughs. This was followed by construction of a second rhyolitic lava dome in the southern fault-bounded trough; meanwhile the boulder breccia-conglomerate continued to accumulate in the northern fault-bounded trough, although it is much thinner than the lower one (0.1 km, Fig. 3), suggesting that accommodation was being filled due to slowing subsidence in the trough. The boulder breccia-conglomerates in the northern fault-bounded trough are dominantly arkosic sandstone matrix, except where they overlie the rhyolitic plinian-phreatoplinian tuffs; there they have the rhyolitic pumice lapilli tuff matrix (Busby and Bassett, in review). The boulder breccia-conglomerates represent proximal debris flow deposits on a highly aggradational fan system, so we do not believe the tuff matrix material was derived from intrabasinal erosion but rather was washed in from surrounding regions that it had mantled.

Unconformity 2 and Sequence 2

Unconformity 2 is shallower than unconformity 1 (0.4 km vertical relief), with slope gradients of less than 20 degrees, and a lateral extent of 2.8 km (Table 1, Fig. 2). Its size and shape make it a possible candidate for a paleocanyon, possibly inherited from the uplift and erosion recorded by unconformity 1.

Sequence 2 records the initiation of creation of accommodation in the southern sub-basin; this was at least 400 m (Table 1). This was accomplished by downdropping the paleocanyon along high-angle faults that step down toward it (Figs. 2, 3). These faults

are clearly syndepositional high-angle reverse faults on the north side of the southern sub-basin, because they pond basal sequence 2 boulder breccia-conglomerate (Fig. 3). The Gringo Gulch fault zone may have also been active, but stratigraphic evidence is obscured by later intrusions plumbed up the fault zone, as well as by unconformities.

Sequence 2 also records continued creation of accommodation in the northern sub-basin (Fig. 3). This was partly accomplished by downdropping of the northern sub-basin along a high-angle fault that developed on the northern margin of the paleohigh, although downdropping may have occurred along the Sawmill Canyon fault zone. Basal sequence 2 strata also thicken into the two grabens within the northern sub-basin, suggesting that the faults there were active, although the strata could have filled relict basins.

Depositional sequence 2 begins with granite-clast, boulder breccia-conglomerate with a red, arkosic matrix, which immediately overlies the sequence boundary in the southern sub-basin (Fig. 3). At the same time in the northern fault-bounded trough of the northern sub-basin, boulder breccia-conglomerates continued to be deposited conformably on sequence 1. These were overlain in both the north and south sub-basins by andesitic ignimbrite erupted from a center that developed at the end of sequence 2 along a syneruptive high-angle fault on the northern margin of the paleohigh that ponded the andesitic ignimbrites (Fig. 3). The fault-controlled andesitic center includes lava flows and sills or small laccoliths (Busby and Bassett, in review).

Unconformity 3 and Sequence 3

Unconformity 3 is a 0.4 km deep unconformity with local slopes up to 20 degrees, a lateral extent of about 3 km (Table 1, Fig. 2), and is restricted to the southern sub-basin

(Fig. 3). It is centered over the paleocanyon defined by unconformity 2 and merges with unconformity 2 over much of the southern subbasin (Figs. 2, 3). This unconformity removed nearly all of the sequence 2 boulder breccia-conglomerate and andesite in the southern sub-basin; they are preserved along the sidewalls of the paleocanyon and in the downdropped grabens north of the paleocanyon on the south flank of the paleohigh (Figs. 2, 3). These downdropped grabens were inactive during deposition of sequence 3 but became reactivated during deposition of sequence 4 (discussed below).

Sequence 3 accommodation was not created by intrabasinal faulting (Figs. 2, 3). The maximum preserved thickness of sequence 3 (300 m, Table 1) is probably a great underestimate of its original thickness in the southern sub-basin, because this is the preserved thickness of it on the paleohigh, and it is largely ignimbrite, which normally thickens into lows. Deposition of sequence 3 therefore probably required several hundred meters of accommodation. This must have been controlled by movement on the Gringo Gulch fault zone on the southern basin margin, since no accommodation was apparently created in the northern sub-basin at that time (i.e. there is no sequence 3 in the northern sub-basin, Table 1).

Basal strata of sequence 3 consists of a distinctive, externally-sourced, rhyolitic crystal-rich ignimbrite (Busby and Bassett, in review), which filled the southern sub-basin and just barely spilled over the paleohigh into the southernmost end of the northern sub-basin (Fig. 3). Fluvial action in the southern sub-basin then reworked the top of the rhyolitic crystal-rich ignimbrite and introduced arkosic sands and granite boulders. Deposition of the lower of the two distinctive rhyolitic red, high-grade ignimbrites followed (Figs. 2, 3); it is only locally preserved beneath unconformity 4. It appears that

the northern sub-basin either had no accommodation space, or all of the sequence 3 strata were effectively stripped from the northern sub-basin during development of unconformity 4.

Unconformity 4 and Sequence 4

Unconformity 4 has 1.2 km of relief with up to 20 degree slopes in the southern sub-basin (labeled 4A, Fig. 3, Table 1), and 0.7 km relief with up to 70 degree slopes in the northern sub-basin (4B, Fig. 3, Table 1). The 70 degree-sloping northern wall in the northern sub-basin was likely controlled by the same fault that was active during deposition of sequences 1 and 2. This makes it possible that growth faulting led to progressive development of the unconformity, and that a 0.7 km high wall never existed at any one time. Unconformity 4 has a 5 km lateral extent (Table 1), and it locally merges with unconformities 2 and 3 in the southern sub-basin (Fig. 2). In the northern sub-basin it cuts down through sequence 2 andesites (as well as completely removing sequence 3, if it was ever deposited there). This represents the only preserved basin-wide unconformity. An unconformity with vertical relief and slope gradients of this scale can only have been produced by tectonic uplift along basin-bounding faults (discussed below).

Accommodation similarly must have been created by tectonic downdropping along basin-bounding faults, because it is so significant in both sub-basins (Fig. 3). Rotation of strata (by about 10 degrees) in the southern sub-basin supports this interpretation. The northern sub-basin is filled with nonstratified proximal rock fall and debris flow deposits, so fanning dips cannot be demonstrated. The preserved thickness of sequence 4 is up to

2.2 km in the southern sub-basin, and up to 0.7 km thick in the northern sub-basin. A minor amount of accommodation was also created within the southern sub-basin by reactivation of four faults bounding syndepositional grabens, because the basal ignimbrite of sequence 3 is offset by those faults, and the upper ignimbrite of sequence 3 overlaps them (Figs. 2, 3; Busby and Bassett, in review). These four faults were high-angle normal faults during sequence two, but they were all reactivated as high-angle reverse faults during deposition of sequence 4.

The basal strata of sequence 4 in the southern sub-basin are the distinctive, externally-sourced, rhyolitic, lithic-rich ignimbrite (Busby and Bassett, in review), which ponded in the southern sub-basin and thinned over the paleohigh, ending abruptly at a high-angle reverse fault on the north margin of the paleohigh (Fig. 3). The rhyolitic, lithic-rich ignimbrite is overlain by thick deposits of andesitic vitric tuff and tuffaceous sandstone that occur in the southern sub-basin only and show paleocurrent directions from the south. We infer that the andesitic pyroclastic debris was supplied from a growing laccolith/cryptodome plumbed along the Gringo Gulch fault zone at the southern margin of the basin, because this cryptodome/laccolith grew into the basin late in the deposition of sequence 4 (Fig. 3). The andesitic vitric tuff and tuffaceous sandstone is in turn overlain by the externally sourced, rhyolitic limestone-lithic ignimbrite (Busby and Bassett, in review). This ignimbrite appears to pinch out northward within the andesitic vitric tuff and tuffaceous sandstone, which also overlies it. Last, the fault-controlled cryptodome/laccolith grew into the basin, while unidentified vents (probably at the southern basin margin) continued to provide andesitic pyroclastic debris to the fluvial systems that deposited the andesitic vitric tuff and tuffaceous sandstone (Fig. 2, 3).

Sequence 4 in the northern sub-basin consists of boulder breccia-conglomerate (about 600 m thick, Fig. 2, 3) with dominantly dacitic lithic tuff matrix and minor arkosic sandstone matrix. This indicates that eruption of the proximal extrabasinal dacitic lava domes had begun, with the debris being reworked into the basin. These boulder breccia-conglomerates are overlain by primary dacitic block-and-ash-flow deposits about 100 m thick (Fig. 2, 3); these may originally have been thicker before they were cut by unconformity 5.

We cannot correlate any lithologic units between the southern and northern sub-basin in sequence 4. In fact, the absence of any ignimbrites in the northern sub-basin (Fig. 3), and the presence of two of them in the southern sub-basin (Fig. 2, 3), suggests to us that accommodation was created at two different times, because ignimbrites are generally widespread; the two ignimbrites thin northward rapidly within the southern sub-basin, however, suggesting that asymmetric subsidence in the south sub-basin effectively ponded the ignimbrites there (Fig. 3). If the two sub-basins did subside at different times, we have no way of determining which one subsided first (Fig. 3).

Unconformity 5 and Sequence 5

Unconformity 5 has 1.8 km of relief, with a lateral extent of 5.5 km (Table 1). Unconformity 5 occurs only in the northern sub-basin (Fig. 2). This unconformity cuts completely through the upper member of the Mount Wrightson Formation (Riggs and Busby-Spera, 1990) along a very steep and high erosional surface. This surface is well exposed, and does not pass downward into a fault cutting the Mount Wrightson Formation (see Fig. 2 of Riggs and Busby-Spera, 1990), so while it may not represent a

fault scarp, it seems remarkably steep for a canyon wall (about 50 degrees slope). Perhaps it represents the scarp of a fault that splays out of the plane of view afforded by the outcrops. Unconformity 5 widened the basin by about 1.5 km (Figs. 2, 3). An unconformity of this scale must record tectonic uplift. The unconformity extends across the northern sub-basin to the paleohigh, and into a correlative conformity in the southern sub-basin.

Accommodation in the northern sub-basin must have been created by tectonic subsidence (probably along the Sawmill Canyon fault zone) because sequence 5 is 1.7 km thick there (Fig. 3). Sequence 5 in the northern sub-basin consists largely of dacitic lithic tuff matrix boulder breccia-conglomerates and dacitic block-and-ash-flow tuffs (Busby and Bassett, in review). Less than 10% of the section consists of arkosic sandstone matrix boulder breccia-conglomerate, indicating a nearly constant influx of dacitic debris. The presence of block-and-ash flow tuffs suggests relative proximity to the collapsing dacite domes, with the most probable location being along the Sawmill Canyon fault zone. These block-and-ash-flow tuffs are lithologically identical to the dacitic block-and-ash-flow tuffs of sequence 4. The block-and-ash-flow tuffs of both sequences are a distinctive part of the basin fill in terms of their relatively high crystal content and color, and they are uniform in terms of textural characteristics and bedding styles (data repository item 2). This would suggest that they record the growth of a monogenetic dome complex, since polygenetic dome complexes are compositionally and texturally heterogeneous (e.g. Mammoth Mountain, Mono-Inyo craters volcanic chain, Bailey, 1989). On the other hand, monogenetic dome complexes probably form over timespans

of thousands of years, which does not seem to allow enough time for the cutting and filling of unconformity 5.

Accommodation in the southern sub-basin region during deposition of sequence 5 appears to have been very small, since the preserved thickness is less than 10 m. Sequence 5 lies conformably upon sequence 4 in the southern sub-basin, and consists entirely of a rhyolitic red high-grade ignimbrite (Busby and Bassett, in review). This is the second rhyolitic, red high-grade ignimbrite in the Glance conglomerate and volcanics. The lower one occurs in sequence 3 in the southern sub-basin only, as described above, whereas the upper one occurs in both the southern and the northern sub-basins (Fig. 2, 3). It thus provides a stratigraphic tie between the northern and southern sub-basins, which became a single basin due to burial of the paleohigh during deposition of sequence 5 (Fig. 3). The upper rhyolitic red high-grade ignimbrite extends across the paleohigh and thickens northward, where it is more strongly welded. It extends about a kilometer further into the northern sub-basin as an ignimbrite, and beyond that the map unit extends another 4.5 km into the northern sub-basin as a layer of 2-3 m ignimbrite blocks in arkosic-sandstone matrix, boulder breccia-conglomerate, as well as in dacitic lithic-tuff matrix, boulder breccia-conglomerate (Fig. 2; Busby and Bassett, in review). This layer of ignimbrite megablocks is mapped all the way to the northernmost end of the basin, at a stratigraphic position about a third of the way from the base of depositional sequence 5, indicating that this part of the massive boulder breccia-conglomerate section has no unconformities hidden within it (Fig. 2).

Unconformity 6 and Sequence 6

Unconformity 6 has 1.5 km relief, with slope gradients up to 55 degrees, and a lateral extent of 5.5 km (Table 1, Fig. 2). Unconformity 6 crosses the former paleohigh (present during sequences 2 through 5) and extends into the former southern sub-basin basin (Fig. 3). It records erosion of any remaining paleohigh, and amalgamation of the two sub-basins into one. The size and shape of unconformity 6 (Fig. 3) suggest tectonic uplift. This is the deepest and steepest-walled intrabasinal unconformity (Table 1).

This unconformity surface is well exposed, and does not pass downward into a fault cutting the Glance conglomerate and volcanics (Fig. 3), so it may not represent a fault scarp, but it seems remarkably steep for a canyon wall (about 50 degrees slope, Table 1). Again, perhaps it represents the scarp of a fault that splays out of the plane of view afforded by the outcrops. If it is the scarp of a growth fault, the scarp need not have been 1.6 km in height at any given time. If it is not a growth fault scarp, its height and steepness indicate that the underlying boulder breccia-conglomerates were lithified at the time. We speculate that early cementation of boulder breccia-conglomerates could have been aided by fluids plumbed up the Sawmill Canyon fault zone; additionally, the tuff matrix of the boulder breccia-conglomerates could have been susceptible to early cementation through zeolitization.

Accommodation for sequence 6 must have been created by tectonic subsidence along the Sawmill Canyon fault zone, because it is very thick (up to 1.5 km) and it thickens toward the fault zone (Table 1, Fig. 3; Busby and Bassett, in review). Lesser accommodation was created by intrabasinal high-angle normal faults (Fig. 3).

Deposition of sequence 6 began with the upper extrabasinally sourced, crystal-rich ignimbrite (data repository item 2; Busby and Bassett, in review). This ignimbrite is

largely cut out by dome intrusions of sequence 6, and is too thin and discontinuous to show on the map (Fig. 2) or the time slices (Fig. 3), but appears on measured sections (Busby and Bassett, in review).

Deposition of the upper extrabasinally sourced, crystal-rich ignimbrite was followed by deposition of intrabasinally-sourced rhyolitic plinian-phreatoplinian tuff across all of the basin (Fig. 2, 3). Rhyolitic plinian-phreatoplinian tuff is only missing in the areas where it is intruded out by succeeding lava domes, and also at the southernmost end of the basin (beyond the eroded paleohigh) where accommodation was low and friable tuffs could have easily been eroded away. The rhyolitic plinian-phreatoplinian tuff locally contains a thin (1 m thick) lithic ignimbrite at its base, which may record vent clearing at the start of the explosive eruption phase.

Deposition of the rhyolitic plinian-phreatoplinian tuff was followed by emplacement of two fault-controlled rhyolitic lava domes (Fig. 3). This records a switch from explosive to effusive eruptive styles within the basin. The two lava domes lie at approximately the same stratigraphic level, and the block-and-ash-flow tuffs that fringe them interfinger with each other (Fig. 3). The southern of the two lava domes overlies a fault that displaces unconformity 6, indicating that it was active during deposition of sequence 6 and probably plumbed the rhyolite to the surface. The southern lava dome was confined to the south by the scarp of this fault. The southern lava dome does not have a direct connection to the rhyolitic intrusion in the cross-sectional view afforded by present-day outcrops, but it lies within a couple of hundred meters of it (Fig. 2, 3). The northern of the two lava domes also does not map directly into the rhyolitic intrusion, but it is connected to it by a syndepositional fault (Fig. 2, 3). This is the same fault that

formed the northern boundary of the southern fault-bounded trough during deposition of sequence 1, with about 1.5 km throw down to the south (Fig. 3). This reactivated fault offsets unconformity 6 by about 200 m, in the opposite sense (down to the north), and the plinian-phreatoplinian tuff at the base of sequence 6 mantles this fault scarp (Fig. 3). Thus the northern fault boundary of the rhyolitic intrusion does not represent rhyolite intrusion downdropped into basement rock; it merely follows the pre-existing fault.

The uppermost part of sequence 6 records a second switch in rhyolitic eruptive styles, this time from effusive to explosive. This began with deposition of the single stratigraphic occurrence of distinctive rhyolitic white high-grade ignimbrite (data repository item 2). This was deposited across the tops of both rhyolitic lava domes and their fringing block-and-ash-flow tuffs (Figs. 2, 3). The rhyolitic white high-grade ignimbrite is up to 40 m thick and fills basal scours less than a meter deep. The rhyolitic white high-grade ignimbrite is cut out by an erosional surface up to 100 m deep (Fig. 2); we have not numbered this as a separate unconformity partly because it has far less relief than the rest of the unconformities in the basin (which have relief of 0.3 – 1.8 km, Table 1), and partly because it, and the sequence above it, are poorly exposed north of the northern rhyolite dome. The sequence above this relatively minor unconformity consists of 1-20 m thick rhyolitic crystal-poor ignimbrites interstratified with rhyolitic plinian-phreatoplinian tuffs largely concentrated in the bottom part of that section.

Depositional sequence 6 is the only depositional sequence in the entire Glance conglomerate and volcanics (including both sub-basins) that has no boulder breccia-conglomerate. This suggests that the rate of volcanic deposition was extremely high,

completely swamping out the background influx of extrabasinally-sourced coarse-grained detritus.

Unconformity 7 and Sequence 7

Unconformity 7 shows a maximum vertical relief of 0.9 km, with slopes up to 40 degrees, and has a lateral extent of 1.5 km (Table 1) before it disappears under the cover of Quaternary gravels (Fig. 2). The unconformity reappears from beneath the gravels in a very small area of outcrop in the southern sub-basin (Fig. 2) where most of sequence 6 is missing, and the basal andesite ignimbrite of sequence 7 rests unconformably on the upper extrabasinally sourced, crystal-rich ignimbrite of basal sequence 6 (described above).

Unconformity 7 is the second intrabasinal unconformity that is steeply asymmetric (south-facing), and it steps southward from the first steeply asymmetric intrabasinal unconformity (unconformity 6). Like unconformity 6, unconformity 7 appears to be an erosional feature rather than a fault scarp because underlying strata are not offset by faults, unless it represents the scarp of a growth fault that spays out of the plane of view afforded by the outcrops. Similar to unconformity 6, the origin of unconformity 7 as an erosional feature requires lithification of the wall rock (in this case, nonwelded ignimbrites rather than boulder breccia-conglomerate) prior to cutting of the unconformity.

Accommodation for deposition of sequence 7 (0.7 km thick, Table 1) must have been largely created by basin-bounding faults, but local intrabasinal accommodation was created by about 100 m offset along a high-angle fault (Figs. 2, 3).

Deposition of sequence 7 began with the andesitic ignimbrite that was ponded in the syn-depositional half graben, but was deposited across the basin (Figs. 2, 3). This is overlain by a continuous andesitic vitric tuff-tuffaceous sandstone unit, only 5 m thick. This in turn is overlain by about 500 m of andesitic vulcanian breccia. Sequence 7 is capped by a rhyolitic crystal-poor ignimbrite that is sheared where it lies along a strand of the Sawmill Canyon fault zone.

Unconformity 8 and Sequence 8

Sequence boundary 8 and depositional sequence 8 (Fig. 2) are truncated by the Sawmill Canyon fault zone (Fig. 2). Unconformity 8 locally merges with unconformity 7 and also appears to be asymmetric, although very little is preserved (Figs. 2, 3). The preserved depth of the unconformity is up to 200 m, and it is filled with boulder breccia-conglomerate with arkosic sandstone matrix.

Syn depositional Faults, Fault Scarps, and Paleo-Slide Scar Scarps

The most important basin-bounding fault zone lay to the north (the Sawmill Canyon Fault Zone, Fig. 1), as shown by the distribution of the boulder breccia-conglomerate lithofacies and by the basin asymmetry (Figs. 2, 3). A less regionally significant fault zone (Figs. 1, 2) with less offset also lay along the south end of the basin, and we name this fault the Gringo Gulch fault zone (Fig. 2, 3). On Drewes' (1971a) map, this E-W trending, subvertical fault zone is cut by the Late Cretaceous Josephine Canyon diorite which intrudes the boulder breccia-conglomerate and dacitic block-and-ash-flow tuff lithofacies defined in our study; therefore we believe his Late Cretaceous age assignment

for the diorite to be correct. Thus, the Gringo Gulch fault zone is a pre-Late Cretaceous (pre-Laramide) fault that bounds the Glance conglomerate and volcanics to the south. Our stratigraphic data from the Glance conglomerate and volcanics indicate that the Gringo Gulch fault zone controlled the southern basin margin and plumbed andesitic volcanic rocks to the surface (Figs. 2, 3).

Intrabasinal faults were clearly active during deposition of sequences 1, 2, 4, 6 and 7 (Fig. 3). The faults are all high-angle faults, some with normal-slip separation (sequences 1, 2, 6 and 7) and some with reverse-slip separation (sequences 2 and 4). Faults that exhibit normal-slip separation were reactivated as faults exhibiting reverse-slip separation (compare sequences 2 and 4), and faults with normal-slip separation were active synchronously with faults showing reverse-slip separation elsewhere in the basin (sequence 2). Alternating reactivation of normal faults as reverse faults, and vice versa, is a distinguishing feature of releasing-restraining bend strike slip basins (Fig. 4). We cannot demonstrate a strike slip component of offset on the faults because our view of the basin is largely two dimensional, so we cannot use piercing points. However, even in present-day, active strike-slip basins it can be difficult or impossible to demonstrate oblique strike slip on high-angle faults with normal- or reverse-slip separation (Wood et al., 1994; Barnes and Audru, 1999; Barnes et al., 2001).

Unconformities 4b, 5, 6, and 7 are highly asymmetric and face very steeply southward, away from the Sawmill Canyon fault zone, with slope gradients of 40-55° and vertical relief of about 1-1.5 km (Table 1, Fig. 3). Only one of these (unconformity 4) can be traced directly downward into a fault (Fig. 2). The steep part of this unconformity may therefore represent a growth fault scarp whose 1.2 km of relief grew incrementally, rather

than representing a paleocliff of that height. The other three steeply asymmetric unconformities do not trace downward into faults (Fig. 2). Although they may represent the scarps of growth faults that splay out of the plane of view afforded by the outcrops, it seems unlikely that three out of four steeply asymmetric unconformities can be explained in this way. Our preferred interpretation is that all four of the steeply asymmetric unconformities represent paleo-slide scar scarps that formed during periods of basin inversion along restraining bends (Fig. 4).

One of the distinguishing features of the basal Bisbee Basin deposits in southern Arizona is slide sheet accumulations. Although some of these are caldera collapse megabreccias in welded ignimbrite (Lipman and Hagstrum, 1992), many more lie within the Glance Conglomerate, and are interpreted to record sliding off syndepositional fault scarps (Hayes and Raup, 1968; Davis et al., 1979; McKee and Anderson, 1998). No previous workers, however, have identified potential paleo-slide scarps for the Glance Conglomerate. We propose that the Glance conglomerate and volcanics in the Santa Rita Mountains preserves paleo-slide scarps. This is consistent with the origin of the formation in a basin along a strike-slip fault, where uplift events created slide scars that were buried during subsidence events, in rapid alternation (Fig. 4).

Departures from Standard Sequence Stratigraphic Models

Currie (1997) proposed a general, now widely-cited sequence-stratigraphic model for nonmarine rocks, where deposition is controlled by changes in basin accommodation. He recognizes three systems tracts: degradational, transitional and aggradational, analogous to the lowstand, transgressive and highstand systems tracts of marine depositional

sequences. Degradational systems tracts overlie sequence-bounding unconformities, and contain the coarsest deposits (conglomerate and sandstone), either contained in incised valleys or as sheets across shallower erosional surfaces. Transitional systems tracts contain more ribbon-like, lenticular sandstone bodies, and aggradational systems tracts contain abundant fine-grained overbank and lacustrine deposits with meandering-anastomosing channel sandstones. In contrast to this model, we see no vertical trends in sedimentary or volcanic styles that we can relate to gradual changes in accommodation. Our systems tracts are all aggradational, reflecting rapid subsidence, and these abruptly alternate with unusually deep unconformities, reflecting rapid uplift.

Standard sequence stratigraphic models for nonmarine basins call upon fluvial incision for creation of the sequence-bounding unconformities. These unconformities show vertical relief of less than 30 m for a single channel, or less than 50 m for an incised valley (Posamentier and Allen, 1997). The erosional surfaces we describe here, in contrast, show 300 to 1800 m of vertical relief. The more symmetrical unconformities (Fig. 2) with lower surface slopes (Table 1) may record cutting of deep canyons at times of basin "pop-up" along basin-bounding strike-slip faults. The asymmetrical unconformities with very high gradients (Table 1) represent fault scarps and slide scars.

Paleosols are commonly used to map unconformities in sequence stratigraphic work, but paleosols appear to be entirely absent from the Glance conglomerate and volcanics. Similarly, paleosols are rare or absent from the classic strike-slip basin, the Miocene Ridge Basin of California (Busby's observations; Link, 2002 in press). Subsidence and sedimentation rates in the Ridge Basin are very high (1 to 2.5 km/m.y.), and this probably explains why there are no well-developed paleosols or unconformities there. High rates

of tectonic subsidence (about 1 km/m.y.) also explains the lack of paleosols in very thick fluvial overbank sequences of the Cretaceous El Gallo Formation, which was deposited in a strike-slip forearc basin (Fulford and Busby, 1993, Busby et al., 1998). We interpret the lack of paleosols in the Glance conglomerate and volcanics to reflect rapid subsidence for each of the eight depositional sequences.

Standard sequence stratigraphic models have been developed for siliclastic and carbonate systems, but this is the first study we are aware of that uses a sequence stratigraphic approach to a volcanically-dominated basin. Departures from the standard models arise from the extreme episodicity of eruptions, which produce voluminous surface deposits of varying erodability. Aggradation is produced by eruptions and does not require any other change in the system (e.g. G. Smith, 1991; R. Smith, 1991), such as the more traditional sequence stratigraphic controls of base level and accommodation. The style of volcanism determines whether the episodic sediment supply is friable and easily remobilized (Fisher and Schmincke, 1984), although climate controls the availability of running water. In the Glance conglomerate and volcanics we find abundant evidence of overland flow and hyperconcentrated flood flow reworking of andesitic tuffs (Fig. 2, 3; data repository item 2; Busby and Bassett, in review). The great thicknesses of the reworked tuffs indicates continual oversupply of friable volcanic sediment.

Another important departure from standard siliclastic or carbonate sequence stratigraphic models is our use of compositional systems tracts in volcanic-volcaniclastic rocks. The fact that silicic and intermediate-composition systems tracts alternate, and do

not interfinger, suggests that magma composition may have been partially controlled by the behavior and geometry of the strike-slip fault, in a manner described by Marra (2001).

TECTONIC RECONSTRUCTION

The Glance Conglomerate and Volcanics in the Santa Rita Mountains: An Intra-Arc Strike-Slip Basin

We interpret the Glance conglomerate and volcanics in the Santa Rita Mountains as the fill of an intra-arc strike-slip basin. Strike-slip basins may be identified by: (1) earthquake focal mechanisms, (2) lateral offset of geological piercing points, or (3) structural style (Barnes and Audru, 1999). Focal mechanisms cannot be used in ancient basins. Piercing points are not available in many strike slip basins; for example, seismic reflection data from active strike-slip basins allows only vertical separation to be quantified (Barnes and Audru, 1999). In most cases, a distinctive structural style is used to identify strike-slip basins (Fig. 4). This style consists of basin bounding strike-slip faults associated with intrabasinal faults with reverse and normal components of slip that develop simultaneously with grabens and arches, in positions that vary rapidly through time (Crowell, 1982; Wood et al., 1994; Nilsen and Sylvester, 1995; Barnes and Audru, 1999; Barnes et al., 2001; Fig. 3 of this study). Our sequence analysis has allowed us to recognize this distinctive structural style in the Glance conglomerate and volcanics of the Santa Rita Mountains (Fig. 3).

Ancient strike-slip basins are most commonly recognized by the distinctive stratigraphic style that is the result of the tectonic “porpoising”, first described by Crowell (1974). Very close spatial and temporal association of releasing bends and

restraining bends results in basin subsidence rates matched by rates of basin inversion and destruction, on a time scale of 10^5 to 10^6 years (Fig. 4; Wood et al., 1994; Barnes et al. 2001). This produces large-scale intrabasinal unconformities, such as those we recognize in the Glance conglomerate and volcanics in the Santa Rita Mountains (Fig. 3). Basin fill is also interpreted to be “recycled” by this mechanism (Barnes et al., 2001). In this paper, we show that this “recycling” can be accomplished largely by landsliding, resulting in a newly recognized type of sequence bounding unconformity that may form in porpoising basins.

When a strike slip fault system is slightly transtensional, the size of the restraining bends is likely to be less than the size of the releasing bends. This can be clearly seen in the modern Hope fault in New Zealand, which has an overall releasing curvature (Fig. 4). Releasing and restraining bends tend to occur in couplets (Fig. 4; Cowan and Pettinga, 1992) with the basins being larger than the pop-up structures. The Hanmer Basin along the Hope Fault has the same couplet structure (Wood et al., 1994). If the restraining bends are of the same scale as the releasing bends, all of the basin fill created at a releasing bend should be inverted and eroded away at the succeeding restraining bend. If the restraining bends are smaller than the releasing bends, however, net subsidence over time will result in partial preservation of the basin fill. This was evidently the case for the Glance conglomerate and volcanics in the Santa Rita Mountains.

We interpret the Glance conglomerate and volcanics to record continental arc volcanism, based on: 1) the large volume of volcanic relative to sedimentary deposits, 2) the wide range in eruptive styles, and 3) the wide compositional range and relative proportions of those compositions (about 30% andesitic, ~25% dacitic, and ~45%

rhyolite volcanic deposits) (Busby and Bassett, in review). This variety of compositions indicates arc volcanism rather than the less voluminous, bimodal compositions more common to continental rifting (Wilson, 1989). Mapping of unconformities and correlation of volcanic systems tracts has enabled us to determine details of eruptive history in an ancient intra-arc strike-slip basin (Busby and Bassett, in review).

The Bisbee Basin: A Strain-Partitioned Arc-Backarc System

Our interpretation of the Glance conglomerate and volcanics as an intra-arc strike-slip basin appears to be in conflict with recently-published models for post-volcanic arc opening of the Bisbee basin (Lawton and McMillan, 1999; Dickinson and Lawton, 2001). Geochemical analyses from basalt lava flows in the Chiricahua Mountains approximately 80 km to the east of the basin described here show no evidence of slab involvement, and are interpreted as continental rift volcanics erupted in a post-arc transtensional borderland (Lawton et al., 1997; Lawton and McMillan, 1999). The basaltic lava flows in the Chiracahua Mountians are interbedded with Glance Conglomerate, but they are far less voluminous and make up a very small proportion of the eastern Bisbee deposits relative to andesitic to rhyolitic volcanics of the western Bisbee basin (Fig. 1). The tectonic model presented in Dickinson and Lawton (2001) calls on slab rollback as the driving force for continental extension in the Bisbee basin (their figures 5 and 8b). However, slab rollback can't exist without subduction (Marsaglia, 1995) which implies the presence of a volcanic arc. If the arc existed, then it would be located on the outboard side of the continental extension. We argue that the Glance conglomerate and volcanics was that arc and that the Bisbee basin was the result of slab rollback and backarc extension (Fig. 5).

Our evidence for intra-arc strike-slip faulting in the Gance conglomerate and volcanics basin suggests that plate convergence was oblique (Jarrard, 1986). Transtensional stresses in the over-riding plate were likely strain-partitioned (McCaffrey, 1992) into the Bisbee basin as a back-arc continental rift behind the Gance conglomerate and volcanics strike-slip continental arc (Fig. 5). In this model, strain partitioning would have allowed coeval back-arc extension and intra-arc strike-slip deformation in the thermally weakened arc axis. In addition, much of the strike-slip motion from the oblique plate convergence could have been taken up by smaller, non-parallel faults (Klute, 1991) in a probably transtensional back-arc Bisbee basin.

Strain partitioning is more commonly discussed for transpressional settings (de Saint Blanquat et al., 1998), but there are examples of strain partitioning in transtensional settings (Acocella et al., 1999; Marra, 2001; Wesnousky and Jones, 1994). Strain partitioning in transtensional settings appears to be controlled by the relative strengths of faults and spatial or temporal changes in the regional stress field (Wesnousky and Jones, 1994). The presence of arc magmatism clearly affects relative fault strengths, especially at depth (de Saint Blanquat et al., 1998), providing the mechanism for strain partitioning in a transtensional convergent margin. We suggest that the Bisbee basin is partitioned into a backarc extensional domain and an intra-arc strike-slip domain represented by the Gance conglomerate and volcanics (Fig. 5).

A possible modern analogue for a strain-partitioned, transtensional arc is the syn-arc back-arc rifting of the Andaman Sea (Curry et al., 1978; Mukhopadhyay, 1984; Maung, 1987). The highly oblique convergence at the Sumatran-Andaman plate boundary shows a number of interesting parallels with our proposed Bisbee basin model (Fig. 5). High

obliquity reduces the volume of volcanism occurring within the arc itself as total rates of convergence decrease. Oblique convergence is strain-partitioned into intra-arc and accretionary wedge strike-slip faults and back-arc transtensional rifts. The back-arc rifting is highly oblique, with basin bounding faults and volcanism obscured by a large sediment supply. Volcanism within the arc includes dome chains erupted along the master strike-slip fault and calderas erupted from strike-slip step-over zones (Bellier and Sebrier, 1994; Bellier et al, 1999). We interpret the Glance conglomerate and volcanics in the western, outboard belt to represent a volcanic arc axis, with intra-arc strike-slip basins equivalent to the northern Sumatran arc; and we interpret the eastern, inboard belt of the Glance conglomerate and volcanics to represent a transtensional backarc basin, equivalent to the southern Andaman Sea.

CONCLUSIONS

We present here the first sequence stratigraphic analysis of a volcanically-dominated basin. We place the cogenetic lithofacies associations of the Glance conglomerate and volcanics into a sequence-stratigraphic framework by mapping eight unconformity- and correlative conformity-bounded sequences across the basin. We use volcanic as well as sedimentary systems tracts to map unconformities through correlative conformities. The unconformities and sequences developed synchronously with high-angle faults with normal- and reverse-slip separation that alternated in space and time, and controlled the positions of grabens and arches. This structural style is typical of alternating restraining-releasing bend strike-slip basins. The unconformity surfaces show extreme vertical relief and most are highly asymmetrical; these are interpreted to be paleo-slide scar surfaces

and lesser paleocanyons. Alternation of slide scars with thick depositional sequences reflects translation of the basin through a series of restraining and releasing bends (“porpoising”), but overall net subsidence of the basin through time suggests that the strike slip fault system as a whole was predominantly transtensional. The use of sequence analysis has allowed greater resolution of basin subsidence and uplift events than would otherwise have been possible, underpinning our intra-arc strike-slip basin tectonic interpretation.

The intra-arc strike slip basin fill is dominated by small polygenetic, multivent volcanic complexes that we consider to be typical of basins sited on a major fault zone, where strands of the fault frequently plumb small batches of magma to the surface. Because of this, individual volcanic constructs do not grow large enough to provide significant accommodation in volcano-bounded basins. We propose a model of strain partitioning along a convergent plate boundary for the opening of the Bisbee Basin in southern Arizona, where the inboard, eastern part represents backarc continental rift basins, and the outboard, western part represents intra-arc strike-slip basins.

ACKNOWLEDGMENTS

We are indebted to Nancy Riggs, Bill Dickinson, Peter Lipman, Ken Hon, Gordon Haxel, Jarg Pettinga, and the late and wonderful Richard Fisher for discussions in the field in southern Arizona and elsewhere. Discussions with Doug Walker and Allen Glazner are also acknowledged. Robert Bothman and Senta provided invaluable field assistance. We sincerely thank Robert and Sandy Bowman for allowing us to stay at their guest house. Support was provided by NSF-EAR 92-19739 awarded to Busby.

REFERENCES CITED

- Acocella, V, Salvini, F, Funicello, R, Faccenna, C, 1999, The role of transfer structures on volcanic activity at Campi Flegrei (southern Italy): *Journal of Volcanology and Geothermal Research*, v. 91; 2-4, Pages, p. 123-139.
- Asmerom, Y., 1988, *Mesozoic Igneous Activity in the Southern Cordillera of North America: Implication for Tectonics and Magma Genesis*, Ph.D. thesis: University of Arizona; 232 pp.
- Asmerom, Y., Zartman, R.E. Damon, P.E. and Shafiqullah, M., 1990, Zircon U-Th-Pb and whole-rock Rb-Sr age patterns of lower Mesozoic igneous rocks in the Santa Rita Mountains, southeast Arizona: Implications for Mesozoic magmatism and tectonics in the southern Cordillera: *Geological Society of America Bulletin*, v. 102, p. 961-968
- Bailey, R.A., 1989, Quaternary volcanism of Long Valley caldera, and Mono-Inyo Craters, Eastern California: 28th International Geological Congress, Field trip Guidebook T313, American Geophysical union, Washington, DC, 36 pp.
- Barnes, P.M., and Audru, J.-C., 1999, Recognition of active strike-slip faulting from high-resolution marine seismic reflection profiles: Eastern Marlborough fault system, New Zealand: *Geological Society of America Bulletin*, v. 111, p. 538-559.
- Barnes, P.M., Sutherland, R., Davy, B., and Delteil, J., 2001, Rapid creation and destruction of sedimentary basins on mature strike-slip faults: an example from the offshore Alpine Fault, New Zealand: *Journal of Structural Geology*, v. 23, p. 1727-1739

- Bassett, K.N., and Busby, C.J., 1996a, Use of ignimbrite stratigraphy for correlation across a regional Mesozoic shear zone: New mapping from S.E. Arizona: Geological Society of America Cordilleran Section Meeting, Abstracts with Programs, v. 28, p. 47
- Bassett, K.N., and Busby, C.J., 1996b, Interstratified rhyolite dome and andesite volcanic deposits in the Late Jurassic(?) Temporal-Bathtub Formations in southern Arizona: Geological Society of America 1996 Annual Meeting, Abstracts with Programs, p. A-114
- Bassett, K.N., and Busby, C.J., 1997, Intra-arc strike-slip basins in the Late Jurassic southern Cordillera: Structural and climatic controls on deposition: Geological Society of America 1997 Annual Meeting, Abstracts with Programs, p. A-201
- Beatty, B., 1987, Correlation of Some Mid-Mesozoic Redbeds and Quartz Sandstones in the Santa Rita Mountains, Mustang Mountains, and Canelo Hills, Southeastern Arizona, M.S. thesis: University of Arizona
- Bellier, O., and Sebrier, M., 1994, Relationship between tectonism and volcanism along the Great Sumatran fault zone deduced by SPOT image analyses: Tectonophysics, v. 233, p. 215-231.
- Bellier, O., Bellon, H., Sebrier, M., and Sutanto, M.R.C., 1999, K-Ar age of the Ranau tuffs; implications for the Ranau Caldera emplacement and slip-partitioning in Sumatra (Indonesia): Tectonophysics, v. 312, p. 347-359.
- Bilodeau, W.L., 1979, Early Cretaceous tectonics and deposition of the Gance Conglomerate, southeastern Arizona, Ph.D. thesis: Stanford University, 145 p.
- Brown, L.F., Jr., and Fisher, W.L., 1977, Seismic stratigraphic interpretation of depositional systems: examples from Brazilian rift and pull apart basins, *in*, Payton,

- C.E., ed., *Seismic Stratigraphy – Applications to Hydrocarbon Exploration*: American Association of Petroleum Geologists Memoir 26, p. 213-248.
- Burns, B.A., Heller, P.L., Marzo, M., and Peola, C., 1997, Fluvial response in a sequence stratigraphic framework: Example from the Montserrat fan delta, Spain: *Journal of Sedimentary Research*, v. 67, p. 311-321
- Busby, C.J., and Bassett, K.N., in review 2002, Facies Model for an intra-arc strike-slip basin; submitted to *Bulletin of Volcanology*
- Busby, C.J., Smith, D.P., Morris, W.R. and Adams, B., 1998, Evolutionary model for convergent margins facing large ocean basins: Mesozoic Baja California (Mexico): *Geology*, v. 26, p. 227-230.
- Busby, C.J., and Kokelaar, B.P., 1992, Development of calderas in a transtensional fault zone: 29th International Geological Congress Abstracts, Kyoto, Japan, v. 2, p. 482
- Busby-Spera, C.J., 1988, Speculative tectonic model for the early Mesozoic arc of the southwest Cordilleran United States: *Geology*, v. 16, p. 1121-1125
- Busby-Spera, C.J., and Kokelaar, B.P., 1991, Controls of the Sawmill Canyon fault zone on Jurassic magmatism and extension/transension in southern Arizona: *Geological Society of America Abstracts*, v.23, p. 250
- Christie-Blick, n., and Biddle, K.T., 1985, Deformation and basin formation along strike slip faults, *in* Biddle, K.T., and Christie-Blick, N., eds., *Strike-slip deformation, basin formation and sedimentation*, SEPM Special Publication 37: SEPM (Society for Sedimentary Geologists), Tulsa, OK, USA, p. 1-34

- Cowan, H.A., 1989, An evaluation of the Late Quaternary displacements and seismic hazard associated with the Hope and Kakapo Faults, Amuri District, North Canterbury, MSc thesis, University of Canterbury, 213 pp.
- Cowan, H., and Pettinga, J.R., 1992, Late Quaternary tectonics and landscape evolution Glynn Wye, North Canterbury, Field Trip Guides, 1992 Joint Annual Conference of Geological Society of New Zealand and New Zealand Geophysical Society, Geological Society of New Zealand Miscellaneous Publication 63B, p. 51-73
- Crowell, J.C., 1974, Origin of late Cenozoic basins in southern California, *in* Tectonics and Sedimentation, SEPM Special Publication v. 22: SEPM (Society for Sedimentary Geology), Tulsa, OK, USA, p. 190-204
- Crowell, J.C., 1982, The tectonics of Ridge basin, southern California, *in* Crowell, J.C., and Link, M.H., eds., Geologic history of Ridge basin southern California: SEPM Series book #22, Pacific Section, Society of Economic Paleontologists and Mineralogists, LA, p. 25-41
- Curry, J.R., Moore, D.G., Lawver, L.A., Emmel, F.J., Raitt, R.W., Henry, M., and Keickhefer, R., 1978, Tectonics of the Andaman Sea and Burma, *in* Watkins, J.S., Montadert, L., Dickerson, P.W., eds., Geological and Geophysical Investigations of Continental Margins: AAPG Memoir 29, p. 189-198
- Currie, B.S., 1997, Sequence stratigraphy of nonmarine Jurassic-Cretaceous rocks, central Cordilleran foreland-basin system: Geological Society of America Bulletin, v. 109, p. 1206-1222

- Dart, C.J., Collier, R.E.L., Gawthorpe, R.L., Keller, J.V.A., and Nichols, G., 1994, Sequence stratigraphy of (?) Pliocene-Quaternary synrift, Gilbert-type fan deltas, northern Peloponnesos, Greece: *Marine and Petroleum Geology*, v. 11, p. 545-560
- Davis, G.H, Phillips, M.P., Reynolds, S.J., and Varga, R.J., 1979, Origin and provenance of some exotic blocks in early Mesozoic red-bed basin deposits, southern Arizona: *Geological Society of America Bulletin*, v. 90, p. 376-384
- de Saint Blanquat, M., Tikoff, B., Teyssier, C., and Vigneresse, J.L., 1998, Transpressional kinematics and magmatic arcs, *in* Holdsworth, R.E., R.A. Strachan, and J.F. Dewey, eds., *Continental Transpressional and Transtensional Tectonics*: Geological Society, London, Special Publication 135, p. 327-340
- Dickinson, W.R., and Lawton, T.F., 2001, Carboniferous to Cretaceous assembly and fragmentation of Mexico: *Geological Society of America Bulletin*, v. 113, p. 1142-1160
- Dickinson, W.R., Klute, M.A., and Swift, P.N., 1986, The Bisbee Basin and its bearing on Late Mesozoic paleogeographic and paleotectonic relations between the Cordilleran and Caribbean regions, *in* Abbott, P.L., ed., *Cretaceous Stratigraphy of Western North America, Field-Trip Guidebook Pacific Section*: SEPM (Society for Sedimentary Geology), p. 51-62
- Dickinson, W.R., Klute, M.A., and Bilodeau, W.L., 1987, Tectonic setting and sedimentological features of upper Mesozoic strata in southeastern Arizona, Fieldtrip guide for 1987 Geological Society of America Meeting: *Arizona Bureau of Geology and Mineral Technology Bulletin*

- Dickinson, W.R., Fiorillo, A.R., Hall, D.L., Monreal, R., Potochnik, A.R., and Swift, P.N., 1989, Cretaceous strata of southern Arizona, *in* Jenny, J.P., and Reynolds, S.J., eds., *Geologic Evolution of Arizona: Arizona Geological Society Digest*, v. 17, p. 397-434
- Dorsey, R.J., and Umhoefer, P.J., 2000, Tectonic and eustatic controls on sequence stratigraphy of the Pliocene Loreto basin, Baja California, Mexico: *Geological Society of America Bulletin*, v. 112, p. 177-199
- Drewes, H., 1971a, Geologic Map of the Mount Wrightson Quadrangle, Southeast of Tucson, Santa Cruz and Pima Counties, Arizona: U.S. Geological Survey Map I-614
- Drewes, H., 1971b, Geologic Map of the Sahuarita Quadrangle, Southeast of Tucson, Pima County, Arizona: U.S. Geological Survey Map I-613
- Drewes, H., 1971c, Mesozoic Stratigraphy of the Santa Rita Mountains, Southeast of Tucson, Arizona: U.S. Geological Survey Professional Paper 748, 35 p.
- Drewes, H., 1972, Structural Geology of the Santa Rita Mountains, Southeast of Tucson, Arizona: U.S. Geological Survey Professional Paper 658-C, 81 p.
- Drewes, H., 1976, Plutonic Rocks of the Santa Rita Mountains, Southeast of Tucson, Arizona: U.S. Geological Survey Professional Paper 915, 75 p.
- Drewes, H., 1981, Tectonics of southeastern Arizona: U.S. Geological Survey Professional Paper 1144, 96 pp.
- Fisher, R.V., and Schmincke, H.U., 1984, *Pyroclastic Rocks*: Springer-Verlag, New York, 472 pp.
- Fulford, M.M., and Busby, C.J., 1993, Tectonic controls on non-marine sedimentation in a Cretaceous fore-arc basin, Baja California, Mexico, *in* Frostick, L.E., and Steel, R.J.,

- eds., Tectonic controls and signature in sedimentary successions: Special Publication v. 20, International Association of Sedimentologists, Blackwell, Oxford Internations, p. 301-333
- Galloway, W.E., 1989, Genetic stratigraphic sequences in basin analysis, I. Architecture and genesis of flooding-surface bounded depositional units: American Association of Petroleum Geologists Bulletin, v. 73, p. 125-142.
- Gawthorpe, R.L., Fraser, A.J., and Collier, R.E.L., 1994, Sequence stratigraphy in active extensional basins; implications for the interpretation of ancient basin fills: Marine and Petroleum Geology, v. 11, p. 642-658
- Hagstrum, J.T., and Lipman, P.W., 1991, Paleomagnetism of three Upper Jurassic ash-flow sheets in southeastern Arizona: Implications for regional deformation: Geophysical Research Letters, v. 18, p. 1413-1416
- Hayes, P.T., 1970a, Mesozoic Stratigraphy of the Mule and Huachuca Mountains, Arizona: U.S. Geological Survey Professional Paper 658-A, 27 p.
- Hayes, P.T., 1970b, Cretaceous Paleogeography of Southeastern Arizona and Adjacent Areas: U.S. Geological Survey Professional Paper 658-B, 42 p.
- Hayes, P.T., and Raup, R.B., 1968, Geologic Map of the Huachuca and Mustang Mountains, Arizona: U.S. Geological Survey Miscellaneous Investigations, Map: I-509
- Jacques-Ayala, C., 1995, Paleogeography and provenance of the Lower Cretaceous Bisbee Group in the Caborca-Santa Ana area, northwestern Sonora, *in* Jacques-Ayala, C., Gonzalez-Leon, C.M., and Roldan-Quintana, J., eds, Studies on the Mesozoic of

- Sonora and Adjacent Areas: GSA Special Paper 301, Geological Society of America, Boulder, p. 79-98
- Jarrard, R.D., 1986, Relations among subduction parameters: *Reviews of Geophysics*, v. 24, p. 217-284
- Jervey, M.T., 1988, Numerical modelling of deposition sequences and their seismic expression, *in* James, D.P. and Leckie, D.A., eds., *Sequences, stratigraphy, sedimentology; surface and subsurface: Memoir v. 15*, Canadian Society of Petroleum Geologists, Calgary, AB, Canada, p.
- Johnson, N.M., Officer, C.B., Opdyke, N.D., Woodard, G.D., Zeitler, P.K., and Lindsay E.H., 1983, Rates of late Cenozoic tectonism in the Vallecito-Fish Creek basin, western Imperial Valley, California: *Geology*, v. 11, p. 664-667
- Klute, M.A., 1991, Sedimentology, sandstone petrofacies, and tectonic setting of the Late Mesozoic Bisbee Basin, southeastern Arizona, Ph.D. thesis: University of Arizona
- Kluth, C.F., 1982, Geology and mid-Mesozoic tectonics of the northern Canelo Hills, Santa Cruz County, Arizona, Ph.D. thesis: University of Arizona, Tucson
- Kluth, C.F., 1983, Geology of the northern Canelo Hills and implications for the Mesozoic tectonics of southeastern Arizona, *in* Reynolds, M.W., and Dolly, E.D., eds., *Mesozoic Paleogeography of the West-Central United States: Rocky Mountain Paleogeography Symposium 2*, Rocky Mountain Section, Society of Economic Paleontologists and Mineralogists, Denver, CO, p. 159-171
- Kowallis, B.J., E.H. Christiansen, A.L. Deino, C. Zhang, and B.H. Everett, 2001, The record of Middle Jurassic volcanism in the Carmell and Temple Cap Formations of southwestern Utah: *Geological Society of America Bulletin*, v.113, p. 373-387

- Krebs, C.K., and Ruiz, J., 1987, Geochemistry of the Canelo Hills volcanics and implications for the Jurassic tectonic setting of southeastern Arizona: *Arizona Geological Society Digest*, v. 18, p. 139-151
- Lawton, T.F., and Olmstead, G.A., 1995, Stratigraphy and structure of the lower part of the Bisbee Group, northeastern Chiricahua Mountains, Arizona, *in* Jacques-Ayala, C., Gonzalez-Leon, C.M., and Roldan-Quintana, J., eds, *Studies on the Mesozoic of Sonora and Adjacent Areas: GSA Special Paper 301*; Geological Society of America, Boulder, p. 21-39
- Lawton, T.F., Garrison, J.M., and McMillan, N.J., 1997, Late Jurassic transtensional borderland on the southwestern margin of North America: *Geological Society of America 1997 Annual Meeting, Abstracts with Programs*, p. A-200
- Lawton, T.F., and McMillan, N.J., 1999, Arc abandonment as a cause for passive continental rifting: Comparison of the Jurassic Mexican Borderland rift and the Cenozoic Rio Grande rift: *Geology*, v. 27, p. 77-782
- Link, M., 2002 in press, Depositional systems and sedimentary facies of the Miocene Ridge Basin group, Ridge Basin, California, *in* Crowell, J.C., ed., *Evolution of Ridge Basin, southern California: An interplay of sedimentation and tectonics: Geological Society of America Special Paper*.
- Lipman, P.W., and Hagstrum, J.T., 1992, Jurassic ashflow sheets, calderas, and related intrusions of the Cordilleran volcanic arc in southeastern Arizona: Implications for regional tectonics and ore deposits: *Geological Society of America Bulletin*, v. 104, p. 32-39

- Marra, F., 2001, Strike-slip faulting and block rotation; a possible triggering mechanism for lava flows in the Alban Hills?: *Journal of Structural Geology*, v. 23, p. 127-141.
- Marsaglia, K.M., 1995, Interarc and backarc basins, *in* Busby, C.J., and Ingersoll, R.V., eds., *Tectonics of Sedimentary Basins*: Blackwell Science, p. 299-330
- Maung, H., 1987, Transcurrent movements in the Burma-Andaman Sea region: *Geology*, v. 15, p. 911-912
- McCaffrey, R., 1992, Oblique plate convergence, slip vectors, and forearc deformation: *Journal of Geophysical Research*, v. 97 B6, p. 8905-8915
- McKee, M.B., and Anderson, T.H., 1998, Mass-gravity deposits and structures in the Lower Cretaceous of Sonora, Mexico: *Geological Society of America Bulletin*, v. 110, p. 1516-1529
- Mukhopadhyay, M., 1984, Seismotectonics of subduction and back-arc rifting under the Andaman Sea: *Marine Geophysical Research*, v. 9, p. 197-210
- Nairn, I.A., Wood, C.P., and Bailey, R.A., 1994, The Reporoa caldera, Taupo Volcanic Zone: Source of the Kaingaroa Ignimbrites: *Bulletin of Volcanology*, v. 56, p. 529-537
- Nilsen, T.H., and Sylvester, A.G., 1995, Strike-slip basins, *in* Busby, C.J., and Ingersoll, R.V., eds., *Tectonics of Sedimentary Basins*: Blackwell Science, Cambridge, MA, p. 425-457
- Nourse, J.A., 1995, Jurassic-Cretaceous paleogeography of the Magdalena region, northern Sonora, and its influence on the positioning of Tertiary metamorphic core complexes, *in* Jacques-Ayala, C., Gonzalez-Leon, C.M., and Roldan-Quintana, J., eds,

- Studies on the Mesozoic of Sonora and Adjacent Areas: GSA Special Paper 301, Geological Society of America, Boulder, p. 59-78
- Posamentier, H.W., and Allen, G.P., 1997, Siliciclastic sequence stratigraphy; concepts and applications: *Concepts in Sedimentology and Paleontology*, v. 7, SEPM (Society for Sedimentary Geology), Tulsa, OK, USA, pp. 204
- Posamentier, H.W., and Vail, P.R., 1988, Eustatic controls on clastic deposition II - Sequence and systems tracts models, *in* Wilgus, C.K., Hastings, B.S., Posamentier, H., Van Wagoner, J., Ross, C.A., and Kendall, D.G.S., eds., *Sea-level changes: An integrated approach: Society of Economic Paleontologists and Mineralogists Special Publication 42*, p. 308-327
- Riggs, N.R., and Haxel, G.B., 1990, The Early to Middle Jurassic magmatic arc in southern Arizona: Plutons to sand dunes, *in* Gehrels, G.E., and Spencer, J.E., eds., *Geologic Excursions Through the Sonoran Desert Region, Arizona and Sonora: Arizona Geological Survey Special Paper 7*, p. 90-103
- Riggs, N.R., and Busby-Spera, C.J., 1990, Evolution of a multi-vent volcanic complex within a subsiding arc graben depression: Mount Wrightson Formation, Arizona: *Geological Society of America Bulletin*, v. 102; p. 1114-1135
- Riggs, N.R., and Busby-Spera, C.J., 1991, Facies analysis of an ancient, dismembered, large caldera complex and implications for intra-arc subsidence: Middle Jurassic strata of Cobre Ridge, southern Arizona, USA: *Sedimentary Geology*, v. 74, p. 30-68
- Riggs, N.R., Mattinson, J.M., and Busby, C.J., 1993, Correlation of Jurassic eolian strata between the magmatic arc and the Colorado Plateau: New U-Pb geochronologic data from southern Arizona: *Geological Society of America Bulletin*, v. 105, p. 1231-1246

- Saleeby, J.B., and Busby-Spera, C.J., 1992, Early Mesozoic tectonic evolution of the western U.S. Cordillera, *in* Burchfiel, B.C., Lipman, P.W., and Zoback, M.L., eds., The Cordilleran Orogen: Conterminous U.S.: The Geology of North America, v. G-3, Geological Society of America, Boulder, CO
- Saunders, A.D., and Tarney, J., 1984, Geochemical characteristics of basaltic volcanism within back-arc basins, *in* Marginal Basins: Geological Society of London Special Publication, v. 16
- Silver, L.T., and Anderson, T.H., 1983, Further evidence and analysis of the Mojave-Sonora megashear(s) in Mesozoic Cordilleran tectonics: Geological Society of America Abstracts with Programs, v. 15, p.273.
- Simons, F.A., 1972, Mesozoic Stratigraphy of the Patagonia Mountains and Adjoining Areas, Santa Cruz County, Arizona: U.S. Geological Survey Professional Paper 658-E, 23 p.
- Simons, F.S., 1974, Geologic map and sections of the Nogales and Lochiel quadrangles, Santa Cruz County, Arizona: USGS Miscellaneous Investigations Series Map I-762
- Smith, G.A., 1991, Facies sequences and geometries in continental volcanoclastic sequences, *in* Fisher, R.V., and Smith, G.A., eds., Sedimentation in volcanic settings: SEPM (Society for Sedimentary Geology) Special Publication No. 45, p. 109-122
- Smith, R.C.M., 1991, Landscape response to a major ignimbrite eruption, Taupo Volcanic Center, New Zealand, *in* Fisher, R.V., and Smith, G.A., eds., Sedimentation in volcanic settings: SEPM (Society for Sedimentary Geology) Special Publication No. 45, p. 123-138

- Titley, S.R., 1976, Evidence for a Mesozoic linear tectonic pattern in south-eastern Arizona: Arizona Geological Society Digest, v. 10, p. 71-101
- Tosdal, R.M., Haxel, G.B., and Wright, J.E., 1989, Jurassic geology of the Sonoran Desert region, southern Arizona, southeastern California, and northernmost Sonora: Construction of a continental-margin magmatic arc, *in* Jenny, J.P., and Reynolds, S.J., eds., Geologic Evolution of Arizona: Arizona Geological Society Digest, v. 17, p. 397-434
- Vail, P.R., and Mitchum, R.M., 1977, Seismic stratigraphy and global changes of sea level; Part 1 Overview, *in* Payton, C.E., ed., Seismic stratigraphy; applications to hydrocarbon exploration, AAPG Memoir 26: American Association of petroleum Geologists, Tulsa, OK, USA, p. 51-52
- van Wagoner, J.C., Posamentier, H.W., Mitchum, R.M. Jr., Vail, P.R., Sraq, J.F., Loutit, T.S., Hardenbol, J., 1988, An overview of the fundamentals of sequence stratigraphy and key definitions, *in* Wilgus, C.K., Hastings, B.S., Ross, C.A., Posamentier, H.W., van Wagoner, J., Kendall, C.G. St.C., eds., Sea-level changes; an integrated approach, SEPM Special Publication 42: SEPM (Society for Sedimentary Geology), Tulsa, OK, USA, p. 39-45
- Vedder, L.K., 1984, Stratigraphic Relationship Between the Late Jurassic Canelo Hills Volcanics and the Glance Conglomerate, Southeastern Arizona, M.S. thesis: University of Arizona, 129 pp.
- Wesnousky, S.G. and Jones, C.H., 1994, Oblique slip, slip partitioning, spatial and temporal changes in the regional stress field, and the relative strength of active faults in the Basin and Range, western United States: *Geology*, v. 22, p. 1031-1034

- Wilson, M., 1989, *Igneous Petrogenesis*: Unwin Hyman, Boston, MA, 466 pp.
- Wood, R.A., Pettinga, J.R., Bannister, S., Lamarche, G., and McMorran, T.J., 1994, Structure of the Hanmer strike-slip basin, Hope Fault, New Zealand: *Geological Society of America Bulletin*, v. 106, p. 1459-1473
- Woodhead, J., Eggins, S., and Gamble, J., 1993, High field strength and transition element systematics in island arc and back-arc basin basalts: Evidence for multi-phase melt extraction and a depleted mantle wedge: *Earth and Planetary Science Letters*, v. 114, p. 491-504

FIGURE CAPTIONS

Fig. 1. Geologic map of part of southern Arizona showing Late Jurassic-Early Cretaceous Bisbee Basin deposits. This map shows the basal Gance Conglomerate and overlying strata of the Bisbee Group, older rocks that acted as sources for the Gance Conglomerate, fault zones that were active in Jurassic time, (including the Sawmill Canyon fault zone), and Jurassic calderas along the Sawmill Canyon fault zone. Late Cretaceous and younger rocks left blank. The box outlines the field area shown in figure 2. Hayes and Raup (1968), Hayes (1970), Drewes (1971a, 1971b, 1971c, 1972, 1976, 1981), Simons (1972, 1974), Titley (1976), Bilodeau (1979), Kluth (1982, 1983), Vedder (1984), Dickinson et al. (1986, 1987, 1989), Beatty (1987), Asmerom (1988), Busby-Spera (1988), Tosdal et al. (1989), Riggs and Haxel (1990); Klute (1991), Riggs and Busby-Spera (1990, 1991),), Busby-Spera and Kokelaar (1991), Busby and Kokelaar (1992), Lipman and Hagstrum (1992), Riggs et al. (1993), and Bassett and Busby (1996a, 1996b, 1997), Busby and Bassett (in review).

Fig. 2. Lithofacies and sequence stratigraphic map of the newly-defined Glance conglomerate and volcanics in the Santa Rita Mountains. The strike and dip of the homoclinal section allows an oblique cross-sectional view of the basin fill. Descriptions and interpretations of lithofacies are presented in Data Repository Item 2 and in Busby and Bassett (in review).

Fig. 3. Evolution of the Glance conglomerate and volcanics, divided into eight time slices defined by unconformity-bounded depositional sequences. Colors for lithofacies map units are the same as those used in Figure 2. Note 2X vertical exaggeration; time slice 8 is identical to our map which is an oblique cut through bedding (Fig. 3). Each time slice includes two major events: (1) cutting of an unconformity (highlighted in blue at the base of the relevant sequence, e.g. unconformity 1 for sequence 1), and (2) deposition of an overlying volcanic and/or sedimentary sequence. Faults that were active during cutting of an unconformity and/or deposition of its overlying sequence are highlighted in blue for that time slice; if the fault(s) became inactive in succeeding time slices, they are shown in black, but revert to blue color in any later time slices in which they were reactivated. The time slices show the movement history of syndepositional high-angle faults, which alternated between normal-slip and reverse-slip separation. Note the controls of syndepositional faults on siting of vents. The time slices also illustrate the fact that cutting of extremely deep, steep unconformities alternated with deposition of very thick depositional sequences, reflecting repeated tectonic uplift and downdropping (“porpoising”) of the basin. Features of the unconformities (depth, steepness, and

lateral extent) as well as the depositional sequences (range in thickness and lateral extent) are given in Table 1.

Fig. 4. Alternating releasing and restraining bends along a strike slip fault, using the Hope Fault in New Zealand as a modern analogue for the Glance conglomerate and volcanics along the Sawmill Canyon fault zone. Releasing and restraining bends produce alternating basins and pop-up structures (after Cowan 1989). As the releasing and restraining bends migrate along the strike of the strike-slip fault, any single location undergoes repeated subsidence and uplift (basin inversion) events, producing basin fill and unconformities. Along the Hope Fault, releasing and restraining bends occur in pairs, separated by long stretches of lesser activity. The Hope Fault is slightly releasing so the restraining bends are smaller than the releasing bends.

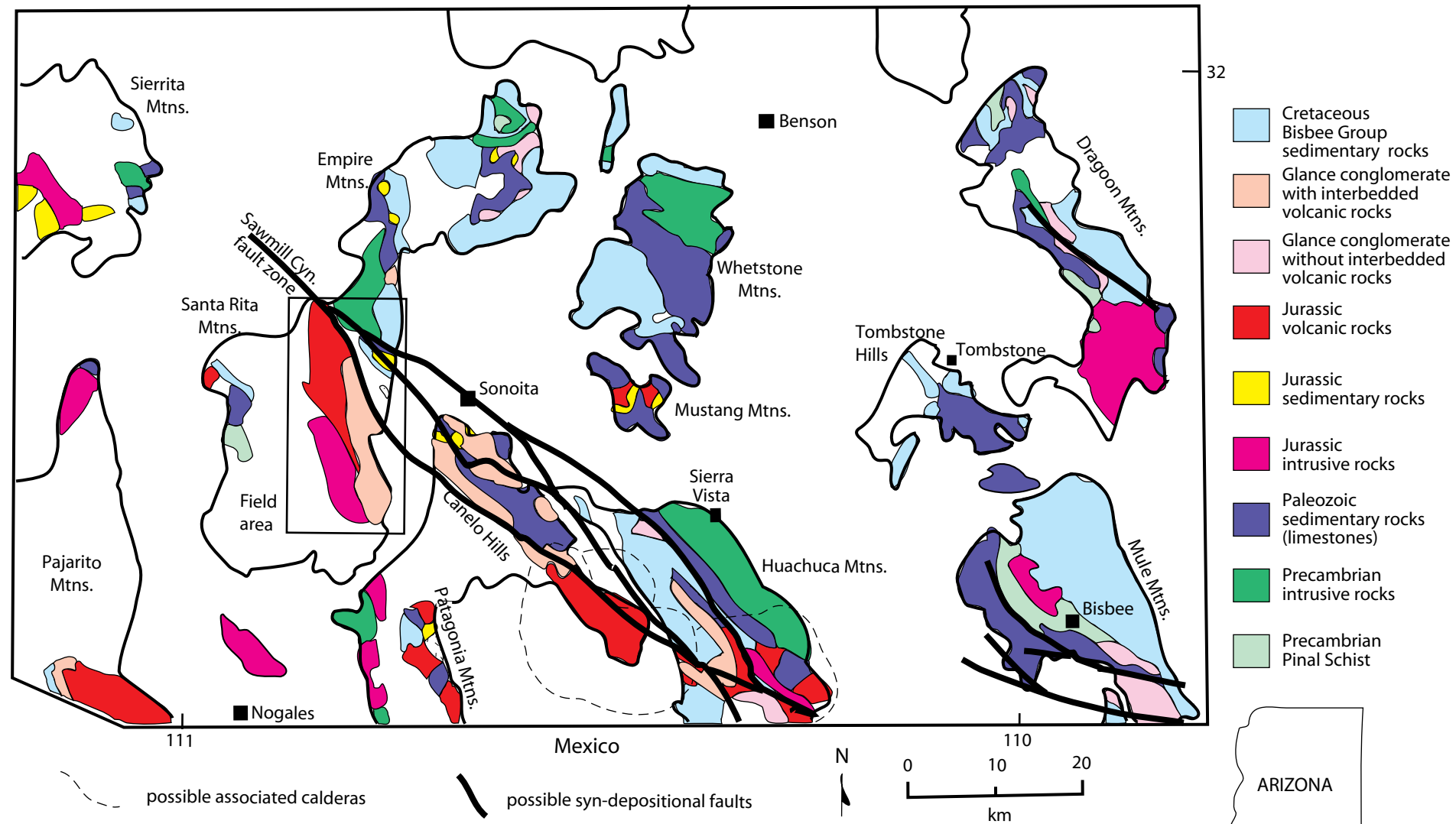
Fig. 5 Regional reconstruction of the Late Jurassic plate boundary in the Cordilleran United States. Strain partitioning along the continental arc caused intra-arc strike-slip faulting along the western edge of the Bisbee basin and backarc transtensional faulting along the eastern edge. A modern analog of the strain-partitioned obliquely convergent plate boundary may lie in Sumatra and the Andaman Sea.

Table 1. A) Surface relief, maximum surface gradients and lateral extents of unconformities in the Glance conglomerate and volcanics. The scale of these require tectonic uplift, by (preserved) intrabasinal and (inferred) extrabasinal reverse faults. B) Maximum preserved thicknesses of the eight unconformity-bound depositional sequences in the Glance conglomerate and volcanics, and their preserved lateral extents. The great thicknesses of these depositional sequences require tectonic

downdropping, by both (preserved) intrabasinal and (inferred) extrabasinal normal faults.

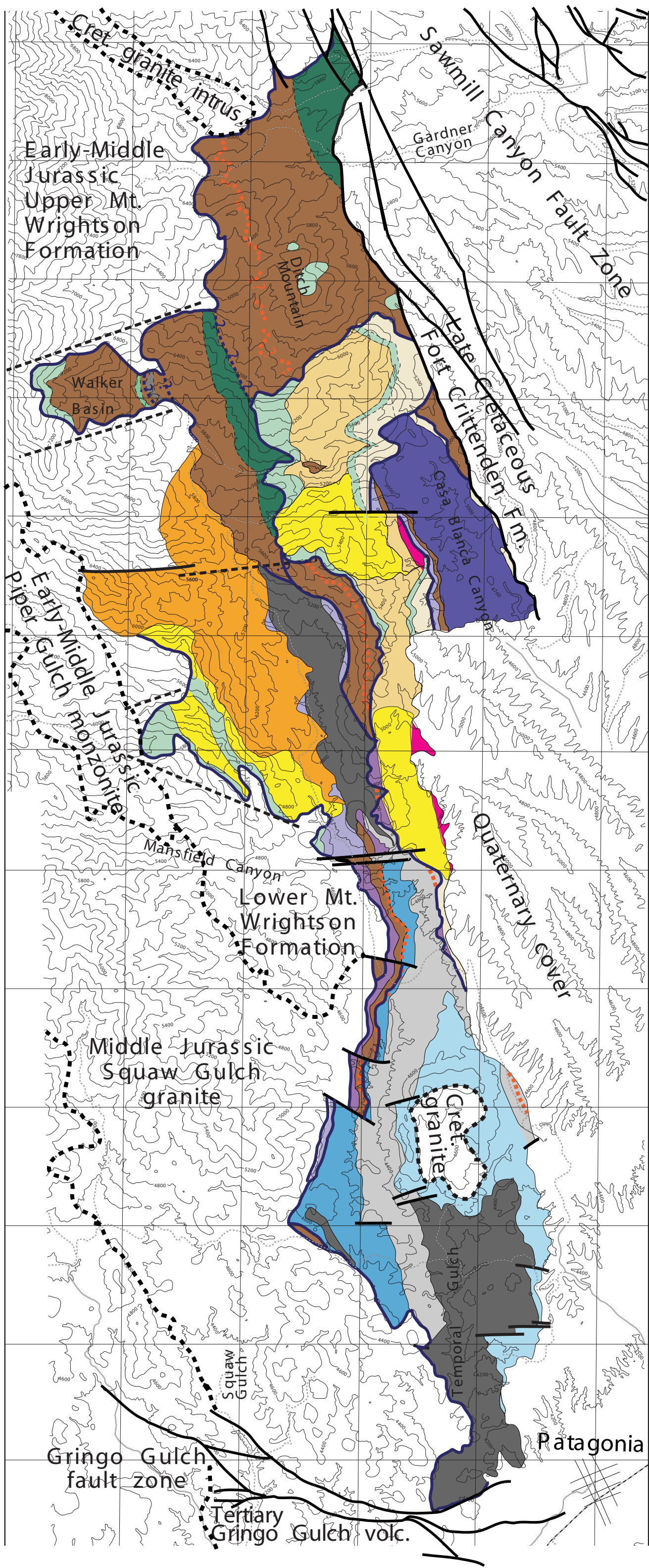
Data Repository Item 1. Remap of the Santa Rita Mountains showing the Glance conglomerate and volcanics. We map major unconformities across all of Drewes' (1971a) original Temporal, Bathtub and Glance Formational and Member boundaries, and the lithofacies repeat and interfinger across Drewes' formational and member boundaries. Distinctive lithofacies of our newly-defined Glance conglomerate and volcanics also occur in parts of Drewes' (1971a) Mount Wrightson Formation and Gringo Gulch volcanics (Fig. 2 and 3); therefore, we include these in the Glance conglomerate and volcanics.

Data Repository Item 2. Table of lithofacies descriptions and interpretations, described in full by Busby and Bassett (in review). Lithofacies are grouped by composition (rhyolitic vs. dacitic vs. andesitic) and inferred source (intrabasinal vs. proximal extrabasinal vs. distal extrabasinal).



Selected Local Geology along the Sawmill Canyon Fault Zone in southern Arizona

Figure 1



Lithofacies Key (not in stratigraphic order due to repetition of facies)

Proximal Extrabasally Sourced

- dacite block & ash flow tuffs
- boulder breccia-conglomerates - undivided

Intrabasally Sourced

- andesitic vulcanian breccia
- andesitic ignimbrite
- andesitic vitric tuffs & tuffaceous sandstones
- andesitic lava flows, flow breccias & intrusions
- rhyolite plinian-phreatoplinian tuffs
- rhyolitic white, high-grade ignimbrite
- rhyolite crystal-poor ignimbrites with minor plinian tuffs
- rhyolite block & ash flow tuffs
- rhyolite dome & dome breccia
- rhyolite hypabyssal intrusions

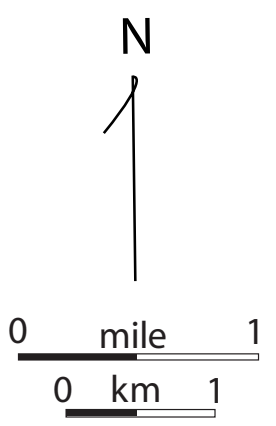
Distal Extrabasally Sourced

- rhyolitic nonwelded crystal-rich ignimbrites
- rhyolitic nonwelded lithic-rich ignimbrite
- rhyolitic welded limestone-lithic ignimbrite
- rhyolite red high-grade ignimbrites

Other

- faults
- unconformity surfaces

regional strike & dip
 30



31° 37' 30"

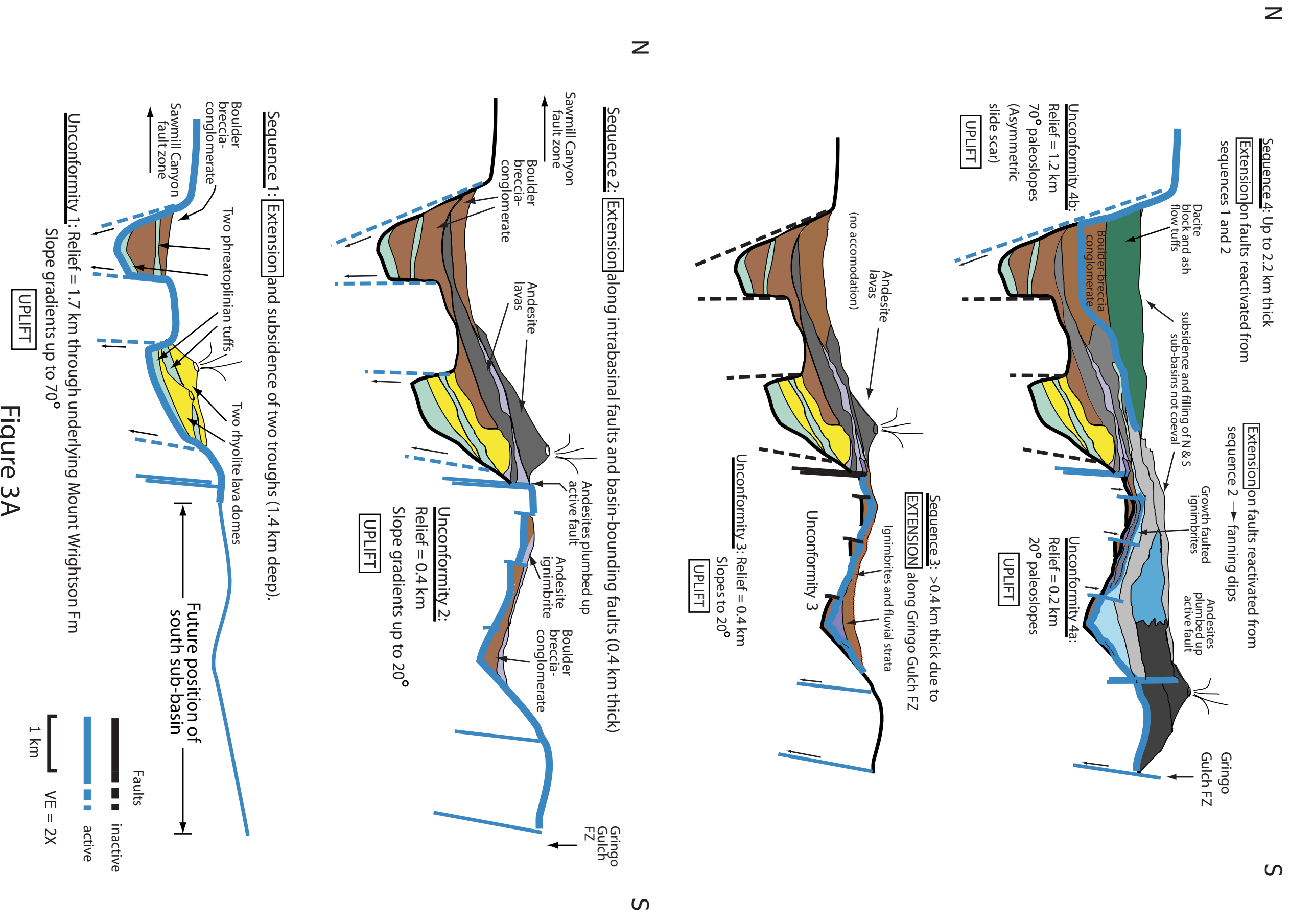


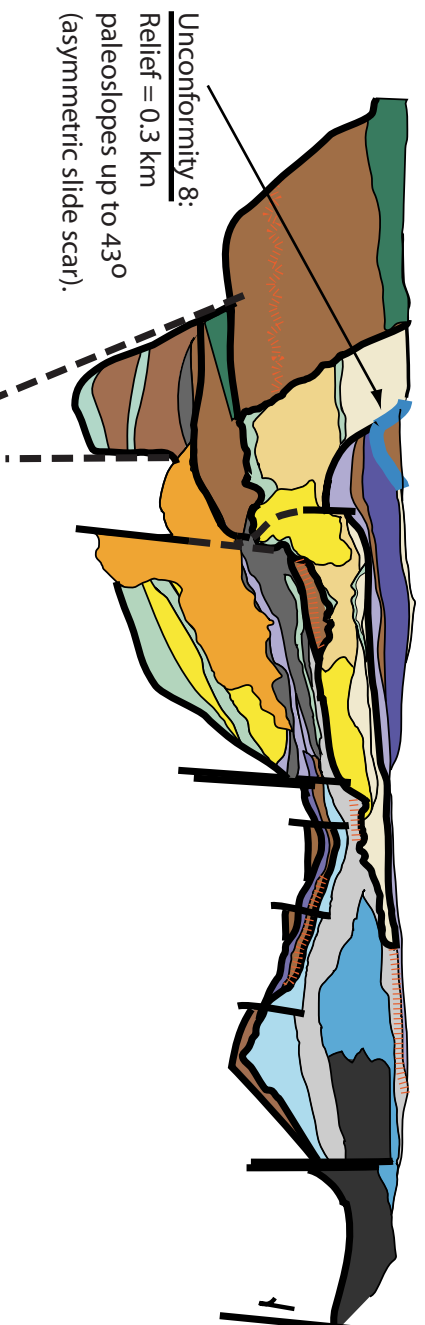
Figure 3A

N

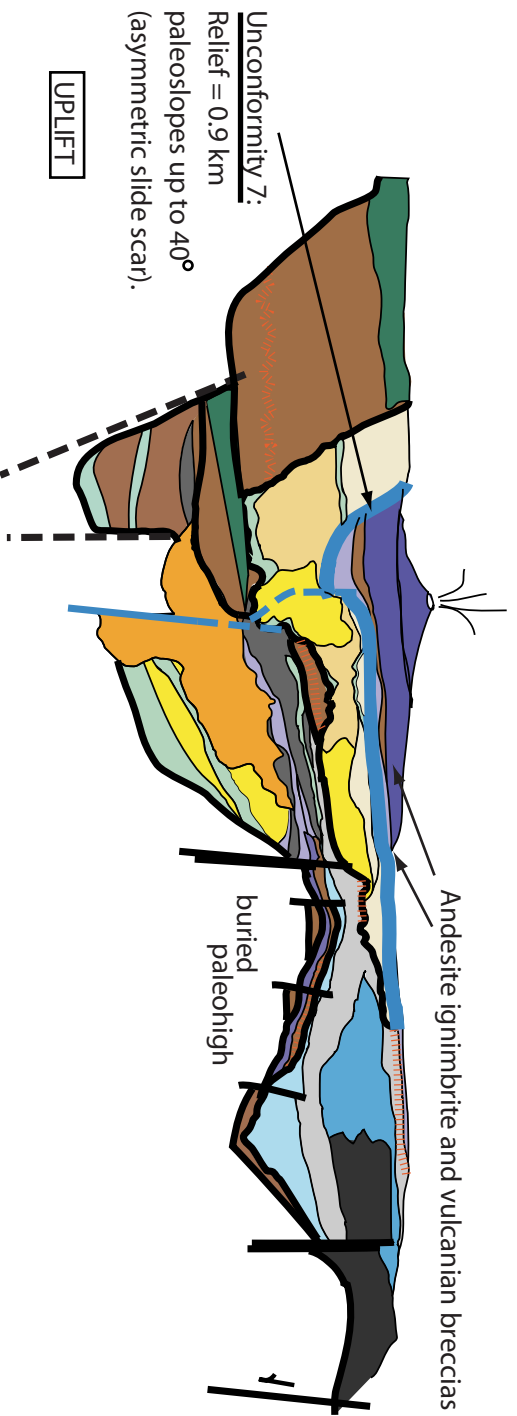
MAP VIEW WITH 2X VERTICAL EXAGGERATION

S

Top sheared by Sawmill Canyon Fault Zone (Laramide reactivation)



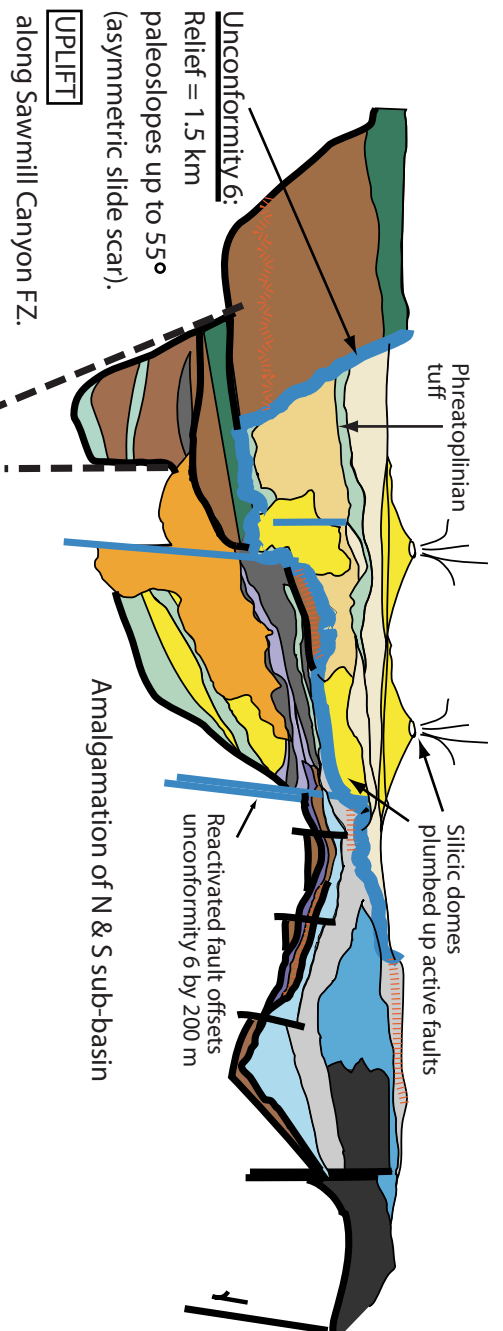
Sequence 7: **EXTENSION** on intrabasin and basin-margin faults (0.7 km thick)



N

Sequence 6: up to 1.5 km thick **SUBSIDENCE** along Sawmill Fanyon FZ. Volcanism swamps out "background" breccia-conglomerate influx.

S



Sequence 5: 1.7 km thick due to **EXTENSION** along Sawmill Canyon fault zone: shedding boulder breccia-conglomerate and plumbing dacite domes

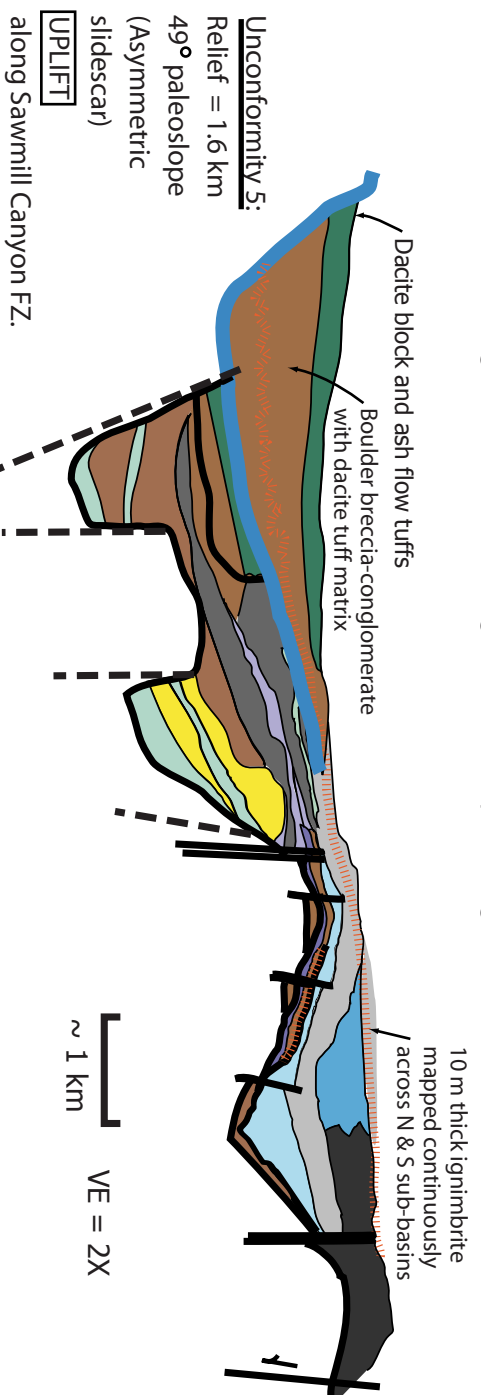
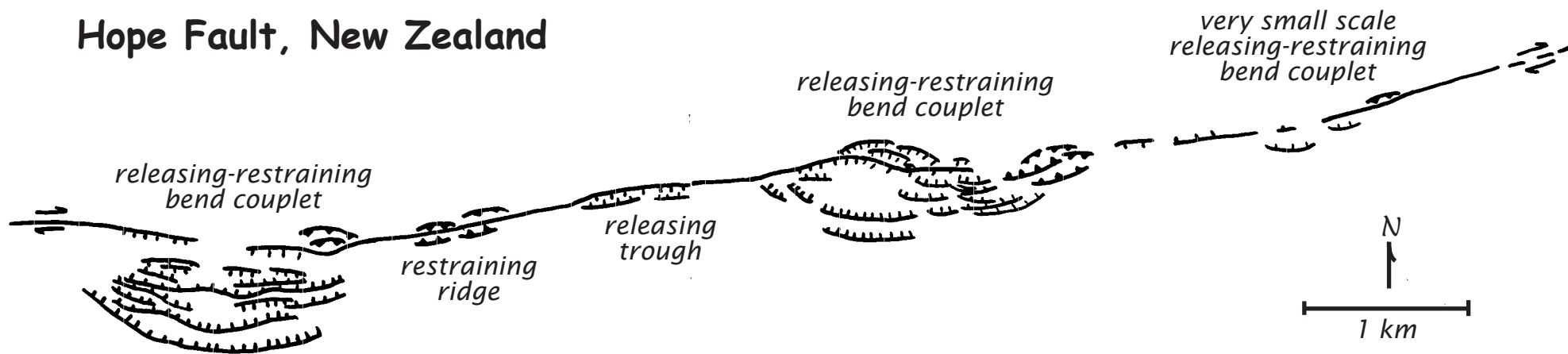


Figure 3B

Hope Fault, New Zealand



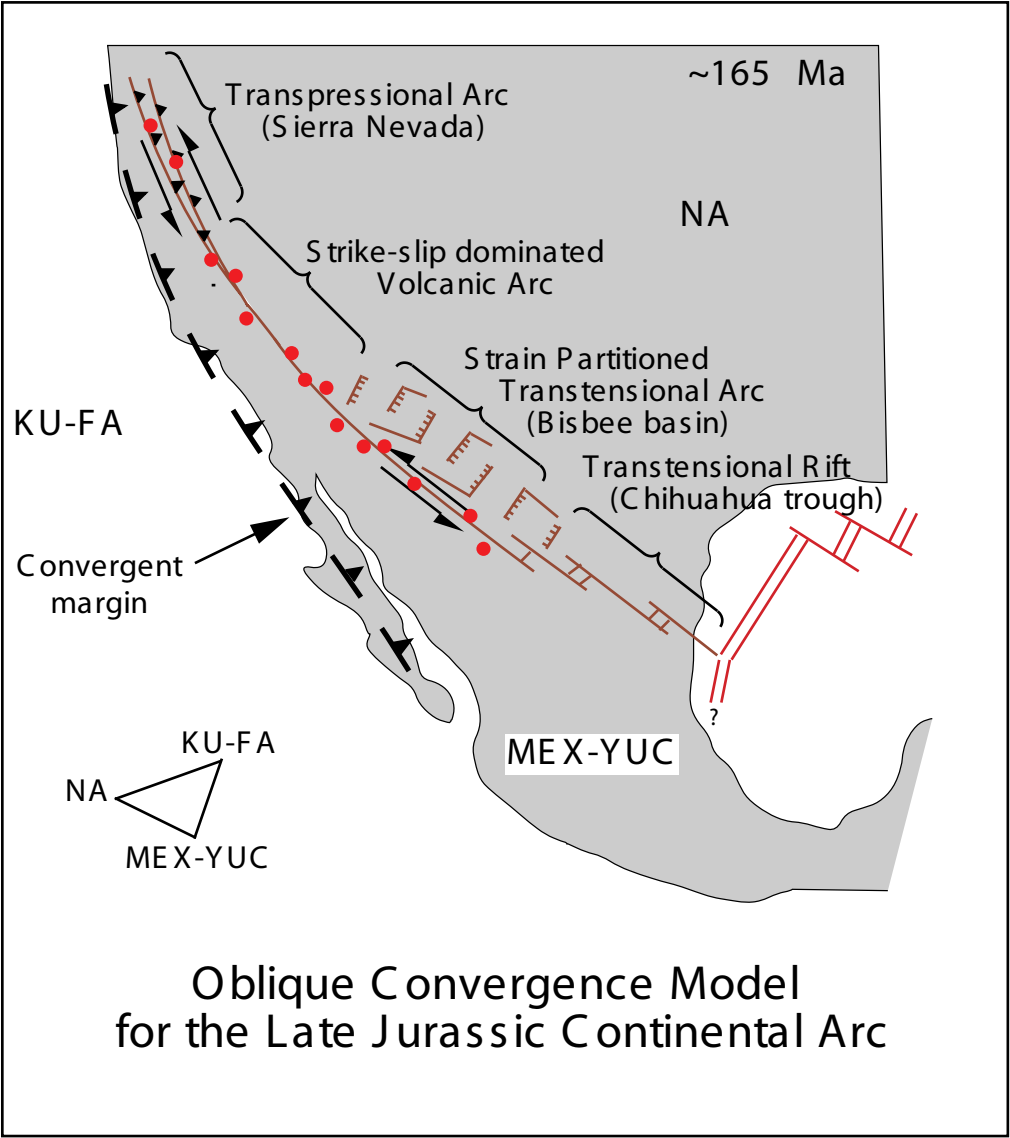
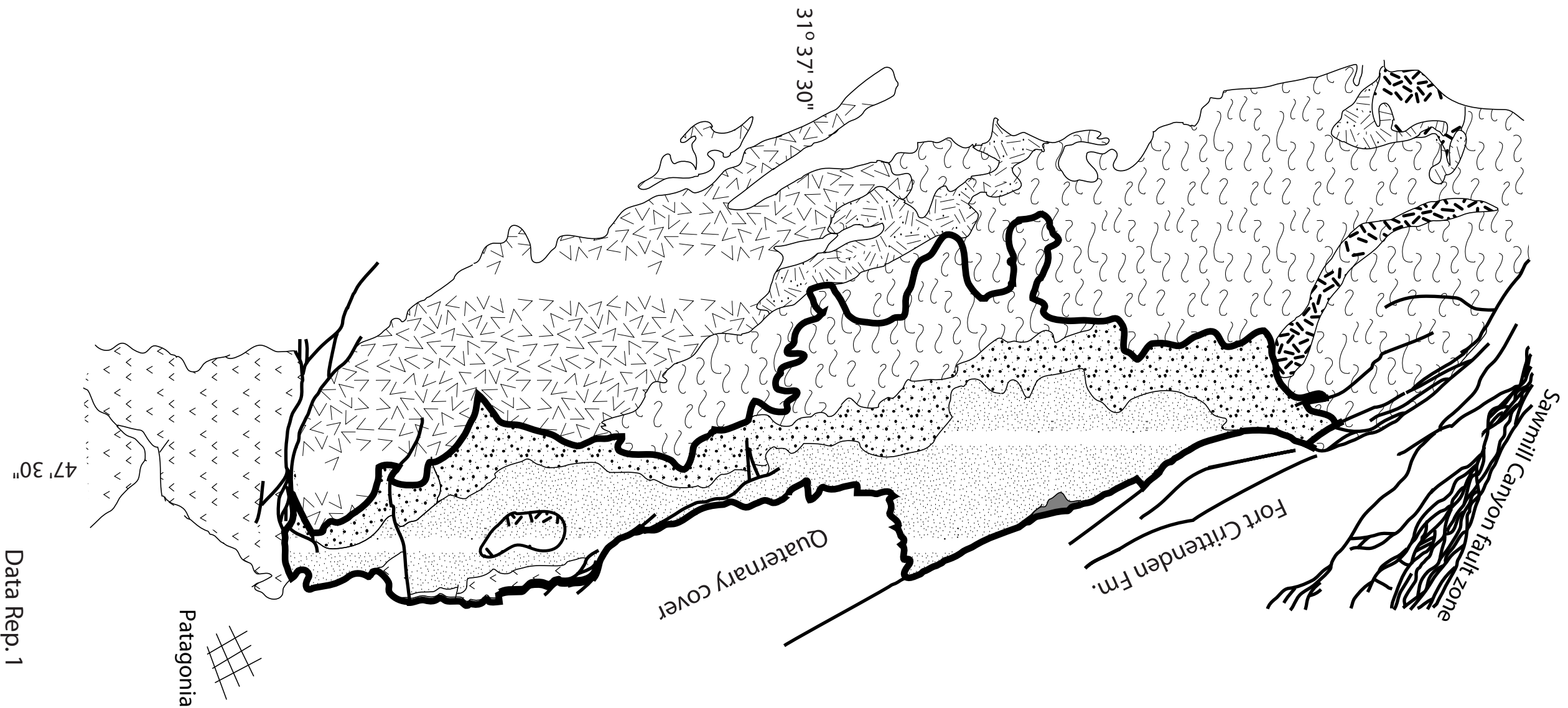


figure 5

<u>Unconformities</u>	minimum relief of surface	maximum slope gradient	lateral extent	Comments
unconformity 1	1.7 km	71 deg.	3.0 km	in N sub-basin, inferred in S sub-basin
unconformity 2	0.4 km	20 deg.	2.8 km	unconf. in S sub-basin, conformable in N
unconformity 3	0.4 km	20 deg.	2.8 km	unconf. in S sub-basin, not present in N
unconformity 4	1.2 km	70 deg.	4.9 km	unconf. in both S & N sub-basins, but not coeval
unconformity 5	1.8 km	48.5 deg.	5.4 km	in northern sub-basin only
unconformity 6	1.5 km	55 deg.	5.4 km	in northern sub-basin only
unconformity 7	0.9 km	40 deg.	1.5 km	in northern sub-basin only
unconformity 8	0.3 km	43 deg.	0.8 km	in northern sub-basin only

<u>Sequences</u>	maximum thickness	minimum thickness	lateral extent	Comments
sequence 1	1.4 km	0.9 km	4.8 km	max in paleohigh, min in N
sequence 2	0.4 km	0.1 km	8 km	max in S, min in paleohigh and N
sequence 3	0.3 km	0.2 km	6.7 km	max in paleohigh, min in N & S (poor preservation)
sequence 4	2.2 km	0.1 km	10.5 km	max in S, min in paleohigh and mid in N
sequence 5	1.6 km	0.03 km	9.1 km	max in N, min in S
sequence 6	1.5 km	0.05 km	5.8 km	max in N, min in S
sequence 7	0.7 km	0.7 km	1.9 km	max in N only
sequence 8	0.3 km	0.3 km	0.8 km	max in N only

Table 1



Drewes (1971) map units

Tertiary Gringo Gulch volcanics

Late Jurassic-Early Cretaceous(?) Glance Conglomerate

Late Jurassic Bathtub Fm.

Late Jurassic Temporal Fm.

Middle Jurassic Mt. Wrightson Fm.

Cretaceous granitic intrusions

Jurassic Squaw Gulch granite

Jurassic Piper Gulch monzonite

included in the newly defined Temporal-Bathtub-Glance (TBGlance) Formation

30 regional strike & dip

N

2 mi.

Patagonia

Data Rep. 1

ROCK NAME	SEQUENCES	FIELD CHARACTERISTICS	THIN SECTION CHARACTERISTICS	FACIES INTERPRETATION
			based on ~400 thin sections	
PROXIMAL	EXTRABASINALLY	SOURCED LITHOFACIES		
boulder breccia-conglomerates	in northern & southern sub-basins; sequences 1, 2, 3, 4, 5, 7, & 8; sequence 8 was previously mapped as Glance conglomerate by Drewes (1971)	massive boulder breccia-cgl.; D99=7-8 m, D50=2-3 m, D50=60 cm; polymict, very angular to sub-rounded clasts of local derivation including red welded rhyolite ignimbrite, limestone, pink granite, kspar porphyry granite, diorite, red siltstone, qtz. arenite, f.g. dacite/rhyolite/andesite volcanics ARKOSIC SANDSTONE MATRIX variety is very poorly sorted, crudely stratified with rare sandstone interbeds & has brick red matrix with dominantly rounded granite clasts; DACITIC LITHIC TUFF MATRIX variety is massive, matrix supported, very poorly sorted & has greenish matrix with dominantly angular f.g. volcanic clasts RHYOLITIC PUMICE LAPILLI TUFF MATRIX variety immediately overlies rhyolitic plinian tuffs in sequence 1 in the northern sub-basin RHYOLITIC QUARTZ PHYRIC PUMICE LAPILLI TUFF MATRIX variety immediately overlies rhyolitic quartz crystal-rich ignimbrite & is reddish/pinkish, poorly-mod. sorted, clast supported, crudely stratified to well-bedded & channelled in m.g. bedded sandstones in sequence 3 in the southern sub-basin	ARKOSIC SANDSTONE MATRIX VARIETY - clasts dominated by granite lithics & few silicic volcanics + siltstone + limestone + qtz. arenite; matrix contains free xls. of kspar, qtz., microcline > biotite, plag. DACITIC LITHIC TUFF MATRIX VARIETY - clasts dominated by f.g. dacite or rhyolite volcanic lithics, minor andesite volcanic lithics + rare limestone, siltstone, granite; matrix contains free xls. of plag. > qtz. RHYOLITIC PUMICE LAPILLI TUFF MATRIX & RHYOLITIC QUARTZ PHYRIC PUMICE LAPILLI TUFF MATRIX - clasts dominated by granite & andesite; matrix contains plag., qtz., volcanic lithics, pumice	talus breccia & avalanche deposition within ~100 m of the fault scarp; proximal to medial debris flow deposition within 3 km of fault zone; distal sheetwash & channelized stream flow within 5 km of fault zone. Clasts all locally derived from outcrop in Santa Rita Mtns. Differences in the matrix determined by availability of volcanic material.
dacitic block & ash flow tuffs	in northern sub-basin only, sequences 4 & 5, but also occurs as matrix to boulder conglomerates in sequences 4 & 5	greenish-gray, massive, monomict tuff breccias; matrix supported; D90<1 m, D50~10-30 cm or D90=30 cm, D50<5 cm; interfingers gradationally with boulder conglomerates	fragmental textures of 75% dense clasts; matrix has broken, smaller xls. relative to dense clasts and moderate to high xl. content suggesting loss of vitric component; 15-30% of 20%plag., 5%qtz., 5% biotite with rare flows containing <5% hb; dense clasts contain lower xl. content relative to matrix; contains rare accidental granite lithics	dacitic block and ash flows probably generated by lava dome collapse at north-eastern basin margin
INTRABASINALLY	SOURCED			
ANDESITIC	LITHOFACIES	ASSOCIATION		
andesitic lava flows, flow breccias & intrusions	sequences 2, 3, 4, & 5	dark gray to black; generally coherent with large plag. xls., commonly flow aligned; locally cross-cuts stratigraphy; locally is flow banded; locally is brecciated & vesicular	varying xl. content 10-50% tot., dominantly of plagioclase, tr.-3% amphibole, <5% Cpx, 3% apatite may be present; locally groundmass is holocrystalline; rare granite accidental lithics introduce Kspar, qtz., titanite	andesitic lava flows, flow breccias and shallow-level intrusions low aspect ratio cryptodomes or laccoliths that locally vent to provided surface lava flow & pyroclastic flows
andesitic ignimbrites	sequences 2, 3, & 7	("wet eruption")	flattened scoria in matrix of bubble-wall shards; xl. rich 35-40% tot. of 30% plag., 5-10% biotite, tr. qtz.; granite accidentals may introduce Kspar; the welded on is less xl.-rich ~10-15% tot.	andesitic pumice-rich pyroclastic flows, non-welded
andesitic vitric tuffs & tuffaceous sandstones	sequences 4, 5 & 7; portions of sequences 4-5 were previously mapped as Gringo Gulch volcanics by Drewes (1971)	lavender-gray to purplish black, textures vary depending on the degree of reworking from VITRIC TUFF to VOLCANIC LITHIC SANDSTONE - very poorly sorted, dark colored sandstone/tuff with angular, andesite grains; largely indistinctly stratified in medium beds; no imbrication; rare small channels of clast-supported, crudely stratified, polyolithic boulder conglomerate similar to boulder conglomerate lithofacies	VITRIC TUFF - ~90% shards, dominantly bubble wall but also platy, blocky, & splintery, & scoria shreds; 10% andesite lithics; xls. of plag., biotite VOLCANIC LITHIC SANDSTONE - andesitic lithics show a range of vesicularity from dense to scoria, with dense clasts dominating the most reworked layers; broken to subrounded xls. of plag. >> biotite >> qtz. > hb.; may have pseudomatrix of squashed & altered pumices	tuffaceous material minimally reworked by fluvial unconfined sheetwash, hyperconcentrated flood flow and channelized traction bedload
andesitic vulcanian breccia	sequence 7 only	dark gray to black, monomict clast-supported tuff breccia in multi-meter thick beds, some with top few decimeters normally graded; dense andesitic clasts, to 1 m in size, with rare granite or aphyric rhyolite accidental lithics; broken plag. & biotite xls. in matrix	generally xl. rich 30-40% tot. but may be as low as 15% tot.; dominantly 30% plag., 5% biotite, <3% hb; mafics generally altered to oxides; dense lithics of same composition as matrix	andesitic vulcanian eruptions - moderate to violent ejection of solid fragments of new lava, generating block-rich avalanches
RHYOLITIC	LITHOFACIES	ASSOCIATION		
rhyolitic intrusions	probable feeder to sequence 6 dome package and intrudes sequences 1, 2, 3	white, aphyric, coherent, with very indistinct flow banding	xl. poor 5-10% tot. of Kspar or plag.>>qtz.; flow banded	rhyolitic shallow-level intrusion feeding upper rhyolite dome package

rhyolitic dome & dome breccias	sequences 1 & 6; portions were previously mapped as Mt. Wrightson Fm. by Drewes (1971)	very white, flow banded, coherent to brecciated with very large clasts (~1 m); may have remobilized pink porcellanite surrounding blocks of dome breccia	very xl. poor to aphyric ~5% tot. of <5% plag., tr. qtz., tr. biotite; f.g. qtz.-fld. mosaic matrix; flow banding common; rare granite accidentals may introduce kspars	rhyolitic lava domes with flow banding, coherent interiors mantled by breccias
rhyolitic block & ash flow tuffs	sequence 6 only	white to pink, monomict tuff breccia; angular dense clasts range in degree of vesicularity from banded rhyolite to rarer pumice; white to pink, aphyric matrix; matrix supported; locally intergradational into white to pink rhyolite ignimbrites	very xl. poor 5-10% tot. of 5-10% plag., tr. qtz., tr. biotite; dense clast blocks in a vitriclastic matrix	rhyolitic block and ash flow deposited lateral to rhyolitic dome breccias, generated by dome collapse
rhyolitic crystal-poor ignimbrite	sequence 6 only	abundant white pumice, commonly flattened, in a pink to white aphyric matrix of vitric tuff; thin (~1 m) lithic-bearing ignimbrites occur locally interbedded with plinian tuffs	xl. poor to aphyric <5% tot. of 1-2% plag., tr. biotite, tr. qtz., tr. Kspar; >95% pumice shreds & shards, shards dominantly blocky or splintery, with lesser bubble wall, locally occurring lithics 2-3 cm	rhyolitic ignimbrite (pumice-rich pyroclastic flow), blocky shards indicate phreatoplinian ("wet") eruption
rhyolitic, white, high-grade ignimbrite	sequence 6 only	white, aphyric with planar to contorted banded (ultrawelded) horizons alternating gradationally with weakly welded horizons showing flattened pumice; ultrawelded horizons show lineations; one locality has aligned tubes (flow structures or log casts?), 10-20 cm diameter, 1-2 m long	aphyric to xl. poor ~5% tot. of <5% plag., <1% qtz., <1% biotite; ultrawelded horizons show extreme plastic deformation of shards and stretching of pumice; moderately welded horizons show sintering of shards and moderate flattening of pumice; bubble-wall shards only, no blocky or splintered shards	rhyolitic high-grade ignimbrite (ultrawelded, pumice-rich pyroclastic flow)
rhyolite plinian-phreatoplinian tuffs	sequences 1, 3, 4, 6 & 7; portions were previously mapped as Mt. Wrightson Fm. by Drewes (1971)	in order of abundance PLINIAN PUMICE FALL DEPOSITS - light greenish-white, pumice lapillistone, commonly thinly tabular-bedded and mantling topography REWORKED PLINIAN FALL DEPOSITS of medium-bedded, erosively-based, lenticular, lithic-enriched & vitric-depleted lapilli tuffs PHREATOPLINIAN FALL DEPOSITS - pinkish red, very thinly tabular-bedded porcellanite (extremely fine-grained tuff); may show convolute lamination & other soft-sediment deformation; also occurs as deformed remnants within dome breccia CRYSTAL-RICH (?) PLINIAN FALL DEPOSITS - plag., qtz., biotite xl. rich, thin tabular beds, some mantling topography, xls. are css sized	PLINIAN PUMICE FALL DEPOSITS - ~80-90% pumice shreds (some long tube), 10-20% bubble-wall shard, aphyric; REWORKED - very xl. poor to 15-20% tot. of 10% qtz., 10% plag.; up to 15% lithics of amygdaloidal andesite, granite, aphyric rhyolite, welded tuff; remainder is pumice PHREATOPLINIAN FALL DEPOSITS - ~80-90% of blocky shards; remainder irresolvably fine grained CRYSTAL-RICH (?) PLINIAN FALL DEPOSITS - xl. rich ~40% tot. of 25% plag., 10% qtz., 5% biotite; remainder ~60% is pumice shreds	PLINIAN PUMICE FALL are widely dispersed sheets of stratified pumice derived from high eruption columns REWORKED PLINIAN FALL scoured bases, lenticularity, loss of delicate vitric components & introduction of lithics indicate remobilization by water PHREATOPLINIAN FALL abundant fines, increased sorting, pronounced bedding & blocky shards indicate interaction of vesiculating magma with surface water producing abundant steam and very fine ash CRYSTAL-RICH (?) PLINIAN FALL DEPOSITS crystal-rich indicates proximal plinian fall
DISTAL RHYOLITIC	EXTRABASINALLY	SOURCED		
rhyolitic crystal-rich ignimbrites	sequence 3 & 6, two occurrences only	white, massive tuff with relict fiamme, xl. rich; qtz. & biotite xls. are large & obvious (css to vcss sized); top locally more pumiceous; rare accidental granite lithics; upper ignimbrite has smaller xls.	xl. rich 30-35% tot. of 15% qtz., 10% plag., 5% biotite, <2% kspars; xls. are large (3-4 mm in sequence 3, 1-3 mm in seq. 6); 70% vitric content of non-welded bubble wall shards & pumice shreds, but generally altered (vapor phase alteration?); feldspars commonly completely calcitized	silicic crystal & pumice rich pyroclastic flow, non-welded
rhyolitic lithic-rich ignimbrite	sequence 4 only	white, massive tuff with well-preserved fiamme; lithic rich ~20-30%; D99=2 m, D90=20-50cm, D50=5 cm; lithics of white tuff, red andesite, siltstone, granite; outcrops in southern paleocanyon completely altered by later andesitic intrusion	xl. poor <15% tot. of plag.>qtz.>Kspar, no biotite; well-preserved nonwelded vitriclastic texture of pumice shreds & bubble wall shards; lithics ~20-30% tot. of andesite & granite with microcline; southern samples completely altered	silicic lithic & pumice rich pyroclastic flow, non-welded
rhyolitic limestone lithic ignimbrite	sequence 4 only; portions were previously mapped as Gringo Gulch volcanics by Drewes (1971)	white to light lavender, massive tuffs with fiamme; xl. poor to aphyric; multiple flow units with welded centers showing more pronounced flattening of pumice; relatively lithic poor but with distinctive compositions including limestone in weakly welded horizons, metamorphosed to marble & amphibolite in welded horizons	xl. poor 5-13% of 10% plag., 3% biotite, tr. qtz.; plag. often completely altered to calcite; bubble wall shards and pumice shreds	silicic pumice rich pyroclastic flows bearing distinctive carbonate & metacarbonate lithics, non-welded to welded in centers of flow units
rhyolitic, red, high-grade ignimbrites	sequences 3 & 5, one in each sequence; upper ignimbrite previously mapped as fault sliver of Mt. Wrightson Fm. by Drewes (1971)	red-maroon tuff with highly elongate fiamme; xl. poor with plag. only; top is spherulitic and blocky; passes laterally to N into unit of 3 m blocks in boulder breccia-conglomerate; resembles older Mt. Wrightson Fm. rheomorphic ignimbrites of Riggs & Busby-Spera (1991)	xl. poor <5% tot. of ~5% plag., tr. biotite>qtz.; more xl. rich in nonwelded outcrop ~15% tot.; vitriclastic texture of faint fiamme in highly welded samples to bubble wall shards in nonwelded samples; sometimes spherulitic, hematized; rare vesicles	silicic pumice rich pyroclastic flows, largely ultrawelded